Desalination and Water Treatment 320 (2024) 100591

Contents lists available at ScienceDirect

Desalination and Water Treatment

journal homepage: www.sciencedirect.com/journal/desalination-and-water-treatment/

A review on sustainable photocatalytic degradation of agro-organochlorine and organophosphorus water pollutants using biogenic iron and iron oxide-based nanoarchitecture materials

Ademidun Adeola Adesibikan[a,b,*], Stephen Sunday Emmanuel[a,*], Sodiq Adeyeye Nafiu[c], Mfeuter Joseph Tachia[d], Kingsley O. Iwuozor[e], Ebuka Chizitere Emenike[e], Adewale George Adeniyi[f,g]

[a] Department of Industrial Chemistry, Faculty of Physical Sciences, University of Ilorin, P. M. B. 1515, Ilorin, Nigeria
[b] Department of Chemistry, Faculty of Natural and Agricultural Sciences, University of Pretoria, Private Bag X20, Hatfield, 0028 Pretoria, South Africa
[c] Department of Chemistry, King Fahd University of Petroleum and Minerals, Dhahran, Saudi Arabia
[d] Department of Aerophysics and Space Research, Moscow Institute of Physics and Technology (MIPT), Russia
[e] Department of Pure and Industrial Chemistry, Nnamdi Azikiwe University, P. M. B. 5025, Awka, Nigeria
[f] Department of Chemical Engineering, University of Ilorin, P. M. B. 1515, Ilorin, Nigeria
[g] Department of Chemical Engineering, Landmark University, P.M.B. 1001, Omu-Aran, Nigeria

ARTICLE INFO

Keywords:
Water insecurity
Organochlorine
Biosynthesized nanoparticles
Iron photocatalyst
Sustainable development goal (SDG)

ABSTRACT

Sustainable accessibility and adequate availability of healthy water are preconditions for healthy living and effective uninterrupted ecological networking. However, the presence of organic pollutants like organochlorine (OC) and organophosphorus (OP) compounds in the environment has led to continuous shrinkage in the percentage of clean water available for humanity's basic needs. Interestingly, green nanoparticles biosynthesized using biogenic entities have recently emerged as an appealing choice for photocatalytic degradation of a wide range of pollutants owing to their eco-benignness. Particularly, biogenic iron-based nanoparticles (BIBNPs) have demonstrated unique properties such as ease of fabrication, excellent regenerability, strong redox potential, the ability to absorb a wide range of visible light, and the ability to produce highly reactive oxygen species that can enhance degradation efficiency and low aggregation which are beneficial for the remediation of water contaminants. The ability of BIBNPs to maintain stability and reactivity under various environmental conditions makes them a promising solution for environmental cleanup efforts. This review aims to critically report and empirically juxtapose the efficiency of biogenic iron and iron oxide NPs for photocatalytic degradation of a wide spectrum of OC and OP pollutants in aquatic environments. The work also generously elucidates the potential of BIBNPs as eco-benign and recyclable photocatalysts for the complete mineralization of OC and OP. The study also pragmatically expounded the photocatalytic degradation mechanism and presented frontiers and future research directions in circular economy, financial analysis, artificial intelligence integration, and hybrid technology. It was discovered that the most prevalent end mineralization products were CO_2 and H_2O, that the least amount of time needed for degradation was just five minutes, and plant extract was the most widely used bioreductant for the bio-fabrication of BIBNPs. The greatest degradation efficiency was also found to be 100 % which is a testament to the superior efficacy of BIBNPs.

1. Introduction

Water is essential for the survival and health of all ecosystems [1,2], thus, protecting it must always be a top priority. However, the alarming water pollution growth has breached water security [3–5]. Today, approximately 4 billion people, or half of the global population, experience extreme water scarcity for at least one month of the year [6–8] and it has been projected that in the next 2 years (2025), it will increase to about 60 to 66 % and may even escalate to 4.8–5.7 billion by 2050 [9,10]. More specifically, the World Water Assessment Program (WWAP) estimates that each year, water pollution kills 100 million people, 1 million aquatic creatures, and 1 million seabirds. It also predicts that by 2025, almost 1000 million people who live in dry regions may face severe water problems[11]. This trajectory escalation is

* Corresponding authors at: Department of Industrial Chemistry, Faculty of Physical Sciences, University of Ilorin, P. M. B. 1515, Ilorin, Nigeria.
E-mail addresses: adesibikana@gamil.com (A.A. Adesibikan), stephenemmanuel6011@gmail.com (S.S. Emmanuel).

https://doi.org/10.1016/j.dwt.2024.100591
Received 15 May 2024; Received in revised form 23 June 2024; Accepted 6 July 2024

due to inevitable rapid industrialization, population growth, and modernization of the agricultural system to control pests, boost crop and animal production, and solve food insecurity problems [12,13]. Without gainsaying, OP and OC are among the major chemicals employed to modernize and boost the agricultural sector(the backbone of the world economy) and control insects that are detrimental to human and animal health[14–16]. Nevertheless, this has made these chemicals pollute the ecosystem when they find their way into the environment, particularly the aquatic bodies through spray drift, transportation from the application site during heavy rains (hundreds to thousand miles), pesticide-filled waste dumping sites, leaching from stockpiles, indiscriminate disposal of the used container, emissions from industrial operations, runoff of agricultural wastage, accidental spills, direct farmyard sewage system discharge during field sprayer filling, cleaning of equipment, indiscriminate disposal of expired or unused or unfinished OP and OC pesticides[17–19]. Notably, the presence of these pollutants in aquatic bodies has led to the degradation of water quality, loss of biodiversity, death of aquatic organisms, disruption of the food chain, interruption of eco-fundamental networking[20–25], and deterioration of human health as they are found to be carcinogenic, mutagenic, teratogenic and even affect endocrine, neuro and reproductive systems[20,26,27]. Thus, the most essential task in this 21st century is to fight the growing water pollution caused by OP and OC for humanity to enjoy their blessing and avert the curse.

Interestingly, several methods including[28–30] ultraviolet radiation, adsorption[31,32], solid phase extraction[33], nanofiltration membrane[33,34], aerobic/biodegradation [35], coagulation [32,33,36,37], ozonation[38], photocatalytic degradation[39–41], and other advanced oxidation processes have been employed remove OP and OC in aquatic environment[20]. Nevertheless, the majority of these methods have several drawbacks, including high costs, drawn-out processes, low efficiency due to OP and OC persistence(remaining in the environment for years), and secondary pollution issues because of the adsorbents' and degraders' inferior cycling capacities [42,43]. Astonishingly photocatalytic degradation—a very economical and environmentally friendly technology—came to light to fully mineralize dangerous organic contaminants like OP and OC into less toxic products and to address the drawbacks of the materials and technologies that were previously in use[43].

It is important to note that degraders and adsorbents are essential to the successful remediation of water pollution. Sadly, some of the materials (clay, kaolin, activated alumina, and activated carbon, among others) employed in photodegradation techniques have shortcomings, including low charge, poor thermal stability, low degradation efficiency/capacity, poor active sites, low photostability, and poor renewability and recyclability [44,45].

Interestingly a better solution to these previously described problems has emerged through the use of Au, Ni/TiO_2, Ag, TiO_2, Fe_3O_4/CdS, Fe, Fe_2O_3, Zn, Cu/ZnO, and other nanoparticles with exceptional surface characteristics, environmental friendliness, catalytic efficiency, and chemical reactivity[46–49]. However, iron-based NPs stood out owing to their excellent recyclability/recoverability, biocompatibility, low toxicity, wide band gap (for iron oxide NPs), ability to absorb a wide range of visible light, ability to produce highly reactive oxygen species, large surface area, and abundance[20,50–52]. However, there are certain hitches to the chemical and physical ways of fabricating metal nanoparticles, including low stability, low curation, poor particle growth, high energy consumption, and the need for a lot of hazardous chemicals. As a result, nanoscientists find it challenging to design new nanoparticles[11,53]. Thankfully, the use of biogenic entities in the production of Fe-based nanoparticles has garnered much attention recently and has been shown to overcome the drawbacks of the physical and chemical techniques, with the added benefit of highly controlled size and shape. Iron nanoparticles are more economical and exhibit lower toxicity to organisms compared to other metal nanoparticles. Additionally, they possess strong redox and adsorption capabilities, making them versatile for various applications across multiple fields such as catalysis, where they improve reaction efficiency; optics, where they contribute to advanced materials; electronics, where they enable the development of novel devices; and environmental remediation, where they play a crucial role in the cleanup of pollutants [54]. Additionally, their cost-effectiveness and broad applicability underscore their potential as a valuable resource in both industrial and environmental contexts and don't call for the use of dangerous chemicals or a lot of energy [11,53–56]. Iron-based biogenic nanoparticles have been extensively studied for their effectiveness in photocatalysis, attributed to their unique properties, including a large specific surface area, magnetic interactions, high surface energy, excellent regenerability, strong redox potential, ability to absorb a wide range of visible light, and the ability to produce highly reactive oxygen species that can enhance degradation efficiency and low aggregation which are beneficial for the remediation of water contaminants [54,57]. These properties allow them to easily agglomerate into micron- or millimeter-sized floccules [58]. They have been reported to function as reductants and catalysts to remove various contaminants, including dyes and chlorinated pollutants [59–61]. Due to their excellent reduction and adsorption capacities, stabilized iron nanoparticles are widely used in environmental remediation, offering a promising solution for the remediation of polluted water, soil, and sediments [62]. Consequently, many biogenic entities have been used to bio-fabricate NPs over time [50,63]. Notably, through an extensive literature survey done by the author, there exist several review works [20,40,70–79,42,80,81,43,64–69] that have been published on photocatalytic degradation of OP and OC using NPs, but no single review work has been directed towards the use of biosynthesized iron and iron oxide based NPs for photocatalytic degradation of OP and OC.

Thus, this present study takes its novelty in being the first review paper on this subject. This review's primary goal is to provide a thorough discussion of the latest empirical trends and cutting-edge studies employing a variety of biogenic iron and iron oxide-based nanoparticles (NPs) for the photodegradation of OP and OC in aquatic environments. Another principal goal of this study is to provide an all-inclusive analysis of the photocatalytic mechanism of biogenic iron and iron oxide-based nanoparticles (NPs) for the degradation of OP and OC pollutants, along with a pragmatic comparison of their photocatalytic efficacy. This work also empirically discussed the regeneration and recyclability of exhausted biogenic iron and iron oxide-based NPs as this is one of the chief motivations for various researchers and industries employing them in pollution remediation. Furthermore, a methodical and objective analysis was conducted on the impact of parametric experimental factors on photodegradation %, including pH, NP dosage, OP and OC concentration, and temperature.

This work also underscores the current and future state of water insecurity up till 2050 and could help scientist and United Nations fasten up their belt on Water Action Agenda and Water Action Decade (2018–2028). Additionally, it is anticipated that the review's section on the health and ecological impact will serve as an assertive reminder to readers in general, especially those employed in labs and industries where OP and OC are used, small- and large-scale farmers, agrochemical workers, and others working in industries where OP and OC are used, to firmly embrace the appropriate safety precautions more than ever before and to fervently ensure proper wastewater treatment instead of the random release of untreated effluent for the general public's safety. Finally, this review also highlighted key challenges and provided an innovative future perspective that is expected to spark fresh ideas in upcoming researchers.

2. Water insecurity

Although the fact that water makes up roughly 71 % of the entire surface of the planet is no longer news [82–84], however, water scarcity is still been identified as one of the largest global risks[85,86] because

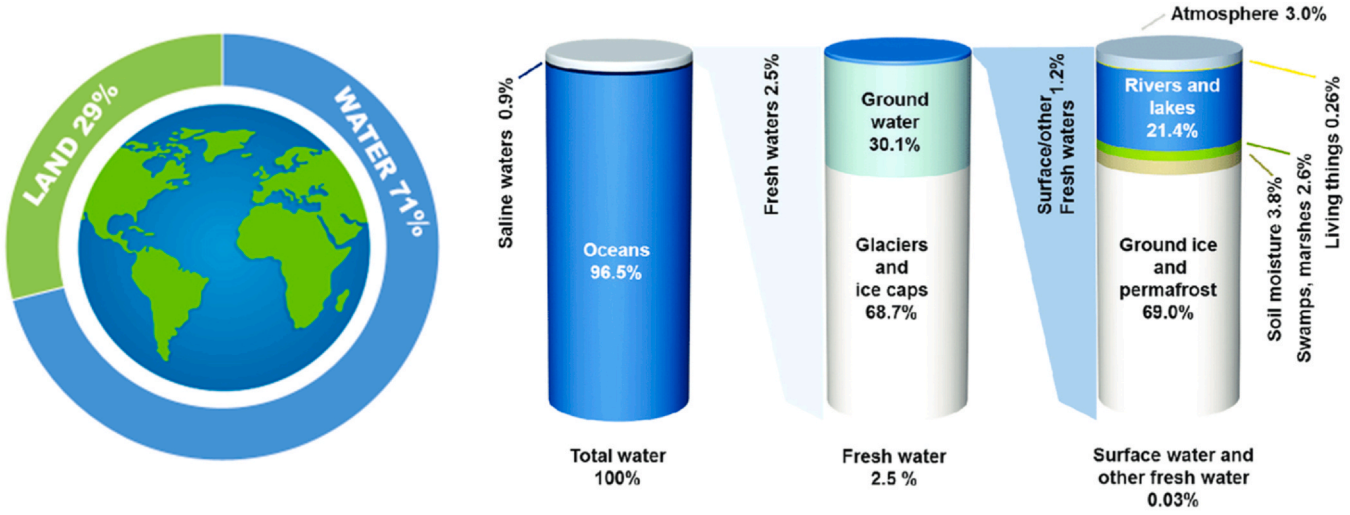

Fig. 1. Water distribution on the planet, displaying the proportion of freshwater and surface water that is available [87].

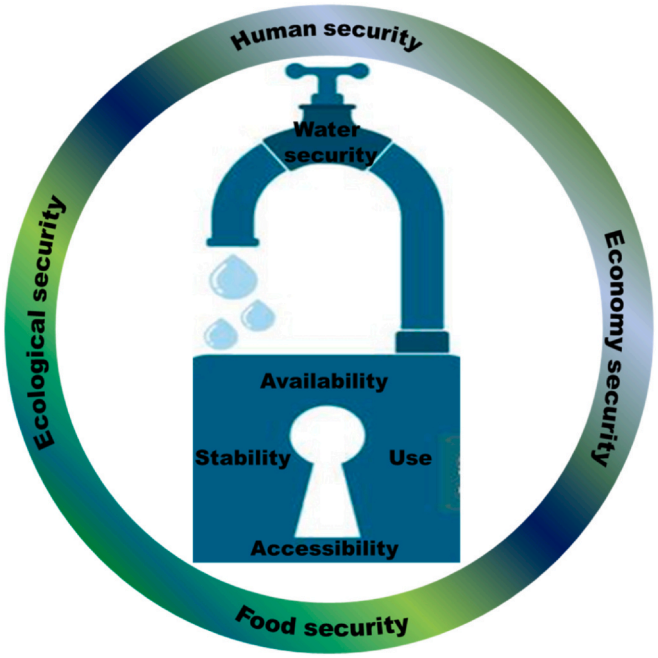

Fig. 2. Four dimensions defining water security.

just 2.5 % of all the water on Planet is regarded as freshwater(Fig. 1) to meet basic demand within the ecological system[82,87] due to the arrival of modernization, fast global industrialization and population growth which has caused water insecurity[17,88,89]. Surprisingly, people still confront water insecurity while consuming just 0.03 % of the fresh water covering the world[11]. Water insecurity, therefore, is distinct from physiological water demands as it encompasses the water required for all earthly occupations and livelihoods [90–92]. Aside from affordability[93], the four dimensions that define water insecurity [90] are shown in Fig. 2 and this includes, availability (physical presence of water and how it is distributed to people) [90,92], accessibility (if there are no obstacles of a physical, financial, cultural, or political nature preventing family members from getting access to adequate water to meet their demands) [90,94,95], use (if the water that is readily accessible and readily available is also suitable, safe to drink, and healthful for non-consumptive uses i.e. free from any form of contamination) [92,93,96], and stability (how consistent are the availability, usability, and accessibility throughout time?) [91,97]. It is imperative to mention that if any of the four domains is compromised, it leads to a state of water insecurity that endangers or threatens well-being, encompassing social, physical, and mental health as well as the ability to engage in vital productive and cultural activities[98–100]. Furthermore, there are ethical considerations surrounding water insecurity[101] as the UN made it clear that access to sanitary facilities and clean drinking water is necessary for the fulfillment of all human rights[102–105]. Furthermore, the significance of water for the growth of humanity and society is highlighted by the 6th SDG (Sustainable Development Goal), which is to "ensure the availability and sustainable management of water and sanitation for all."[92,101].

Statistically, according to the Global Water Security 2023 Assessment [106], 3 out of every 4 people, or 78 % of the world's populace (6.1 billion), currently reside in nations with inadequate access to water. It was further accentuated that the number of deaths caused by inadequate access to clean drinking water, sanitation, and hygiene services surpasses that of water-related disasters[106–109]. In fact, according to the World Health Organization 2023 water report[110], an estimated 502,000 deaths from diarrhea alone are attributed to polluted drinking water annually. It was also envisaged that around two-thirds of the world's inhabitants will continue to live water-insecure well beyond 2030 if radical actions are not taken now with all alacrity[106]. In addition, the overall water demand is steadily increasing by one percent yearly and rivalry for water by the triangulated sectors shown in Fig. 3**b** will worsen more than ever, as the world's entire populace is anticipated to reach 9.8 billion by 2050 and 11.2 billion by 2021 as shown in Fig. 3**a** [10,111,112]. The above-highlighted worldwide widespread water insecurity thus conveys its 6usignificance irrefutably[92] and calls for urgent attention as it may be impossible for water bodies to replenish naturally themselves due to the alarming climate change effect.

3. Sources and mobility of OP and OC in aquatic bodies

Typically, the major way that OC and OP enter into the environment is through the use of agricultural pesticide sprays[113]. Notably, only 0.1 % of sprayed OP/OC targets pests; the remaining 99.9 % move far and near across numerous environmental matrices and reach humans, as seen in Fig. 4. Thus, the primary point sources in the environment are the places where their utilization is still practiced [113,114]. In particular, OC/OP can be detected hundreds to thousands of kilometers from the application location since it can travel a great distance through the wind before depositing on soils and water [115,116]. As shown in Fig. 4**,** during application, after volatilizing out of the soil, OC and OP are suspended in the atmosphere before being redeposited. Additionally, they might be absorbed by plants or seep into the earth, contaminating groundwater[116,117].

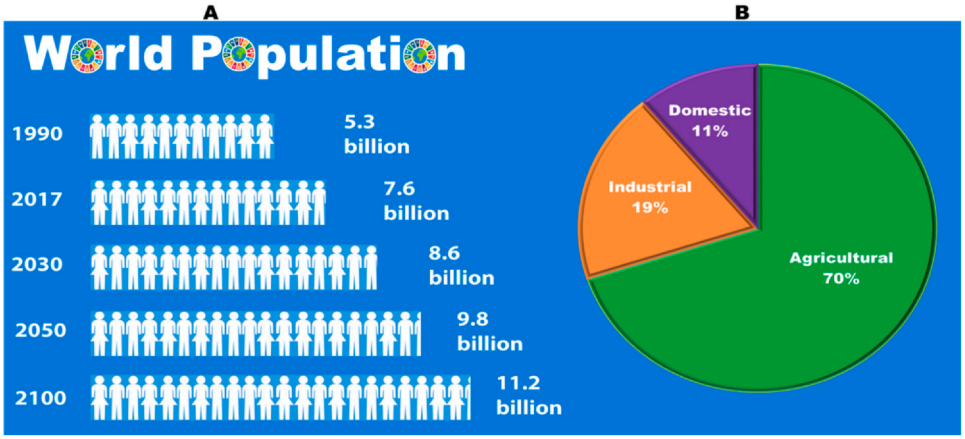

Fig. 3. (A) World population growth trend, (B) sector-wise use of freshwater across the globe.

Specifically, the use of OP and OC pesticides can contaminate the aquatic environment in several ways, such as spray drift, transportation from the application site after rain, indiscriminate disposal of used containers, emissions from industrial operations, direct farmyard discharge into sewage systems during field sprayer filling, and more, runoff, leaching from stockpiles, pesticide-contaminated waste dumping sites, runoff of agricultural wastage, accidental spills, cleaning of equipment, indiscriminate disposal of expired or unused or unfinished OP and OC pesticides[18,118,119]. Additionally, soil runoff from OP/OC-containing waste disposal sites and soil-air exchange, which allows the pollutants to volatilize from the soil into the atmosphere, can carry these pollutants into aquatic bodies and return them to the soil[113,120], water via air-water exchange[113], and direct industrial ejections[19,113]. Pesticides in aquatic environments can desorb or adsorb on suspended materials before sinking to the bottom and settling there, where they then bioaccumulate in fish and other aquatic life [116]. Notably, research has shown that OP/OC contaminants get to humans largely through water and food, especially fish and vegetables because they are commonly eaten by a lot of people and have no cultural or religion rebuff[116,121].

4. Global ecological, and health impact of OP and OC

The widespread use and persistence of OP and OC compounds have made their pollution a significant global issue as well as having a profound environmental and public health challenge on a global scale [122]. By and large, both acute and chronic disorders are among the many health and environmental risks brought on by OP and OC pollution[19,123]. Because they are deadly to some groups of organisms, they can have extremely negative effects on certain environmental niches, such as water, as well as other habitats [123]. From a global perspective, it is important to note that a mere 0.1 % of applied OP and OC pesticides effectively hit target pests. The remaining 99.9 % disperses into various environmental matrices, resulting in significant water quality degradation, adversely affecting non-target organisms, and contributing to a considerable loss of biodiversity, particularly within aquatic ecosystems [19,114,123]. Additionally, reports from the World Health Organization (WHO) in the early 1990s estimated that around one million unintentional organochlorine and organophosphorus pesticide poisonings occurred annually, resulting in

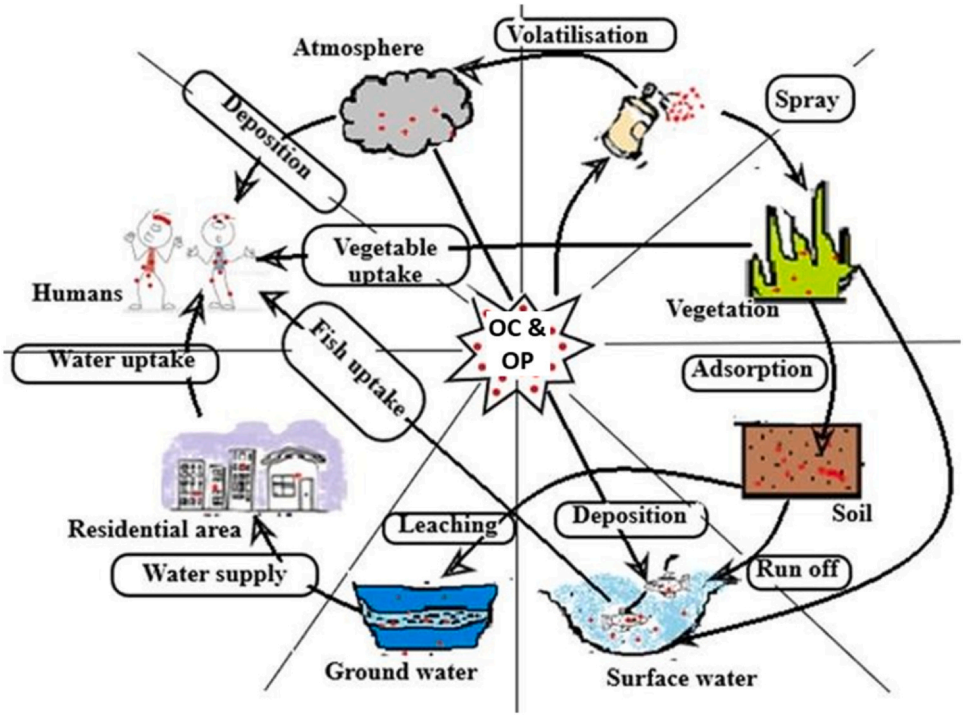

Fig. 4. Transportation of OP and OC to humans within the environment[114].

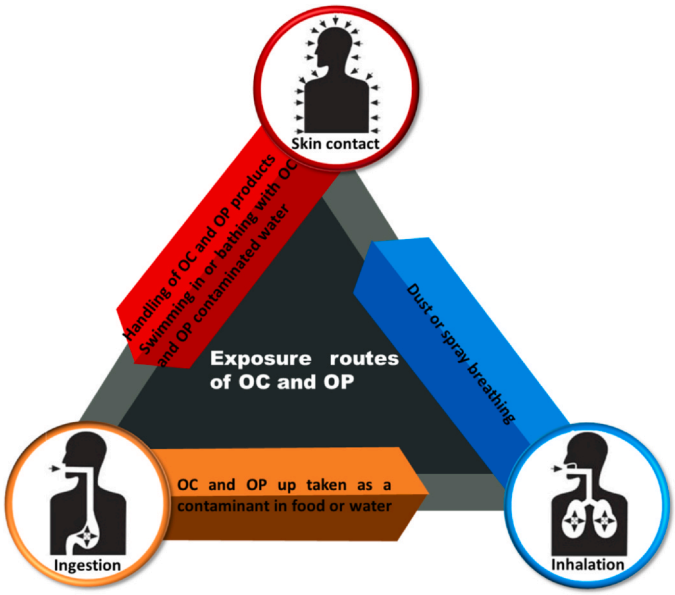

Fig. 5. Exposure routes of organochlorine and organophosphorus to humans.

approximately 20,000 deaths per year globally. However, in recent years, these figures have drastically increased to over 150,000 people per annual worldwide [124,125]. More specifically, 44 % of farmers fall victim to these tragic deaths yearly on a global scale [126].

Furthermore, regarding aquatic lives, fish may be directly impacted by OC and OP, with smaller fish being more affected than bigger fish [127]. Pesticides can also have indirect harmful impacts on fish by reducing the amount of algae and plankton that fish eat, altering their eating preferences, and degrading the integrity of fish habitat. Some OC and OP may severely affect and decrease the profusion of primary producers like zooplankton, micro-crustaceans, etc., and thus ultimately decrease the primary and secondary consumers[128,129]. Some of the negative impacts the OP and OC have on the aquatic faunas comprise renal tubule necrosis, aberrant behavior, secondary lamellae curling, respiratory strain, irregular swimming, prolonged metamorphosis, glomerulus contraction and disturbance of the hepatic system [130,131].

From the biomagnification standpoint, higher predators, including humans, have been shown to have extremely high levels of OP and OC pollutants in their tissues and other organs as a result of larger species eating fewer living things as they go up the food chain[132,133].

In addition, there also exists an indirect eco-economical impact of OP and OC through bioaccumulation because the chief receptor for these pollutants is fat tissue and thus accumulates in fish fats. When humans consume eatable fish and fish tissue contaminated by fat-soluble OC like DDT, it gets to the human adipose tissues and begins mayhem in the body[127,134]. Therefore, human exposure to OC and OP through the consumption of polluted fish and shellfish may have an effect on economies since the survival of fish that reside at the bottom of the primary agriculturally submerged portions of the ocean is dependent upon it[135,136].

Notably, In addition to immune system deficits and inborn defects, the effects of OC and OP on humans are often linked to pulmonary dysfunction, and hematological morbidity[127,137]. However, the ecological impact as per physiological effects includes reproductive failure or inhibition (includes decreased testicular weights, decreased sperm potentiality, spermatogenesis suppression, sperm DNA damage, and an upsurge in the generation of abnormal sperm)[138,139], disruption of the endocrine system[19,140], death, immune system suppression, cancers(breast, lung, and prostate), tumors, and wounds on animals and fishes[137,141–144], obesity[19], occurrence of type 2 diabetes[145,146], teratogenic effects and cardiovascular toxicity [127,147], DNA, cellular mutilation, poor fish health is observed through a low red-to-white blood cell ratio, severe mud on fish gills and crusts, etc., and eggshell weakness[127]. Also, mild exposure to OP and OC has been attributed to unintentional muscle contraction, nausea, impaired vision, chronic muscle spasms, dizziness, headache, and irritation[130,148]. Moderate exposure is commonly accompanied by symptoms such as vomiting, palpitations, trembling in the muscles, diarrhea, disorientation, and copious amounts of mucus[130].

In addition, convulsion, complete collapse, sluggish pulse, disorientation, profuse tears, mucus and saliva, and coma are signs of significant exposure to these OPs[130]. The majority of the aforementioned effect is because when OP/OC found their way into the human body tissues (adipose tissue, breast milk, and blood), they accumulate in fat tissue, gradually degrade, and stay in human bodies for quite a while[19,116]. Furthermore, the induction of peroxisome proliferator-activated receptors, alteration of calcium signaling, and lipid metabolism are the main ways that exposure to OCPs in breast milk impairs an infant's brain development[149,150]. Exposure to OCPs impairs thyroid hormones by imitating their action, which reduces the hormone's effectiveness and harms the brain, nerves, and reproductive systems in humans. In women, OCPs are particularly known to cause spontaneous miscarriages, early births, ovarian issues, and hormone problems [151,152]. Furthermore, these contaminants can enter the mother's bloodstream during pregnancy, travel to the placenta, and then disrupt its ability to produce and release hormones and enzymes, transport nutrients, and produce waste, disrupting fetal development and the last stages of placental life[116,153]. Exposure to OP and OC has also been associated with changes in the urogenital tract's development, growth of “Lewy bodies”, hypertension, Alzheimer's disease, hepatitis, ATP synthesis disruption, pulmonary fibrosis, asthma, cough, multiple myeloma, brain cancer, and sore throat [19,154,155]. In summary, the death caused by OP and OC via any of the routes shown in Fig. 5 is becoming higher than that caused by common diseases as reports have it that out of millions of people exposed to these pollutants yearly, a very alarming death rate of 0.4 % to 1.9 % follow[125,134,156].

5. Synthesis of the biogenic Iron and Iron oxide NPs

By and large, the bio-fabrication of iron and iron oxide nanoparticles using biogenic entities is accomplished through a bottom-up approach [53,157]. Notably, the iron-based NP biosynthesis method can be broadly divided into two, namely phyto-genic synthesis and

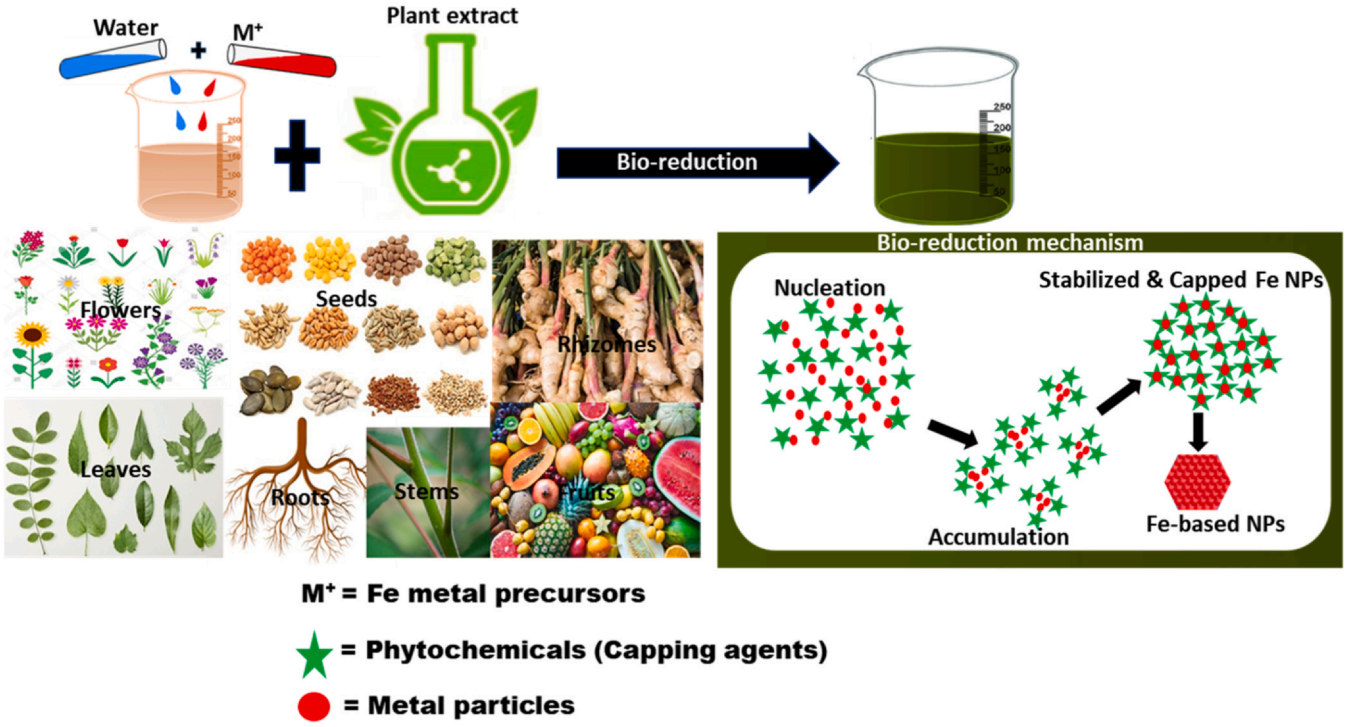

Fig. 6. Overview of phyto-genic synthesis of Iron nanoparticles[53].

microbial synthesis [53]. These approaches not only minimize the environmental impact but also enhance the biocompatibility, and afford the nanoparticles more important function groups and thus broadening their potential applications in areas such as environmental remediation, and catalysis.

6. Phytogenic synthesis of Iron and Iron oxide nanoparticles

Iron and Iron oxide nanoparticles are formed by the reduction of metal ions in the presence of a suitable reducing agent and a capping agent, typically phytochemicals found in the plant extract as shown in Fig. 6. The process generally involves three phases: the activation phase, which involves the breakdown of the precursor; the nucleation or growth phase; and the termination phase, which is the decline phase that determines the final morphology of the nanoparticles [53,87]. The metal salt is gradually added to the plant extract with constant gentle stirring until nuclei begin to form. The size and shape diversity of the synthesized nanoparticles (NPs) depend on the composition and concentration of the bioactive molecules present in the plant extract [158]. The key factors influencing the nucleation and stabilization of plant-mediated nanoparticle (NP) formation include the pH of the reaction solution, the concentration of reactants, reaction time, temperature, metal salt concentration, and extract concentration. These variables not only control the initial formation and stability of the NPs but also significantly impact the overall quality, size, and morphology of the synthesized Iron and Iron oxide NPS. Adjusting these parameters can lead to the production of Iron and Iron oxide NPS with specific characteristics tailored for various applications [53,87,159]. In addition, a few limitations that need more attention in future research. Firstly, standardization issues: The chemical makeup of plant extracts may vary greatly depending on the species, growth environment, harvesting period, and extraction techniques used. Because of this heterogeneity, it is challenging to standardize the synthesis process, which results in inconsistent yield, size, and shape of the nanoparticles[87,160]. Secondly, the purity of nanoparticles can be sometimes questionable because numerous biomolecules have been found in plant extracts; some of these biomolecules may stick to the biogenic NPs and compromise their functioning and purity. Thus, additional purification is required to obtain high-purity NPs, which might, in turn, increase the complexity of the phyto-genic method. Thirdly, extensive and careful optimization of reaction conditions is often required to achieve desired NP characteristics[82]. Lastly, scalability is still a challenge and requires urgent attention.

7. Microbial synthesis of Iron and Iron oxide nanoparticles

The formation of microbial iron-based NPs occurs through either an intracellular or extracellular pathway. In the intracellular pathway, metal ions are transported into the microbe's cell where cellular enzymes facilitate their reduction. Conversely, in the extracellular pathway, metal ions adhere to the cell's surface and are reduced by enzymes present outside the cell [161]. Extracellular mechanisms are particularly advantageous for the recovery of NPs, enhancing the practicality and efficiency of the biogenic synthesis approach. The hydroxyl groups present in the polysaccharides of both microalgae and macroalgae play a critical role in the reduction and stabilization of iron-based NPs. Additionally, membrane-bound oxidoreductases and yeast-derived quinones act as effective bio-reductants in this process [53,161]. Additionally, as illustrated in Fig. 7, the intracellular bio-production of iron-based NPs involves the participation of NADH and NADH-dependent nitrate reductase enzymes. These enzymes play a crucial role in the reduction process, facilitating the conversion of metal ions into nanoparticles within the cellular environment. The involvement of NADH, a key coenzyme in cellular metabolic processes, underscores the intricate biochemical interactions that drive the synthesis of iron-based NPs. In extracellular bio-preparation, nitrate reductase-mediated fabrication plays a key role. Here, iron NPs are synthesized by reductase enzymes either embedded in the cell wall or secreted into the growth medium. This process involves nitrate reductase or metabolites converting metal ions into their zero-valent form, facilitating the formation of nanoparticles outside the cellular environment [162].

Notably, the mycogenic NP synthesis method faces some salient challenges in the area of selecting the mycogenic entities, controlling resulting NP morphology so as not to take the morphology of the

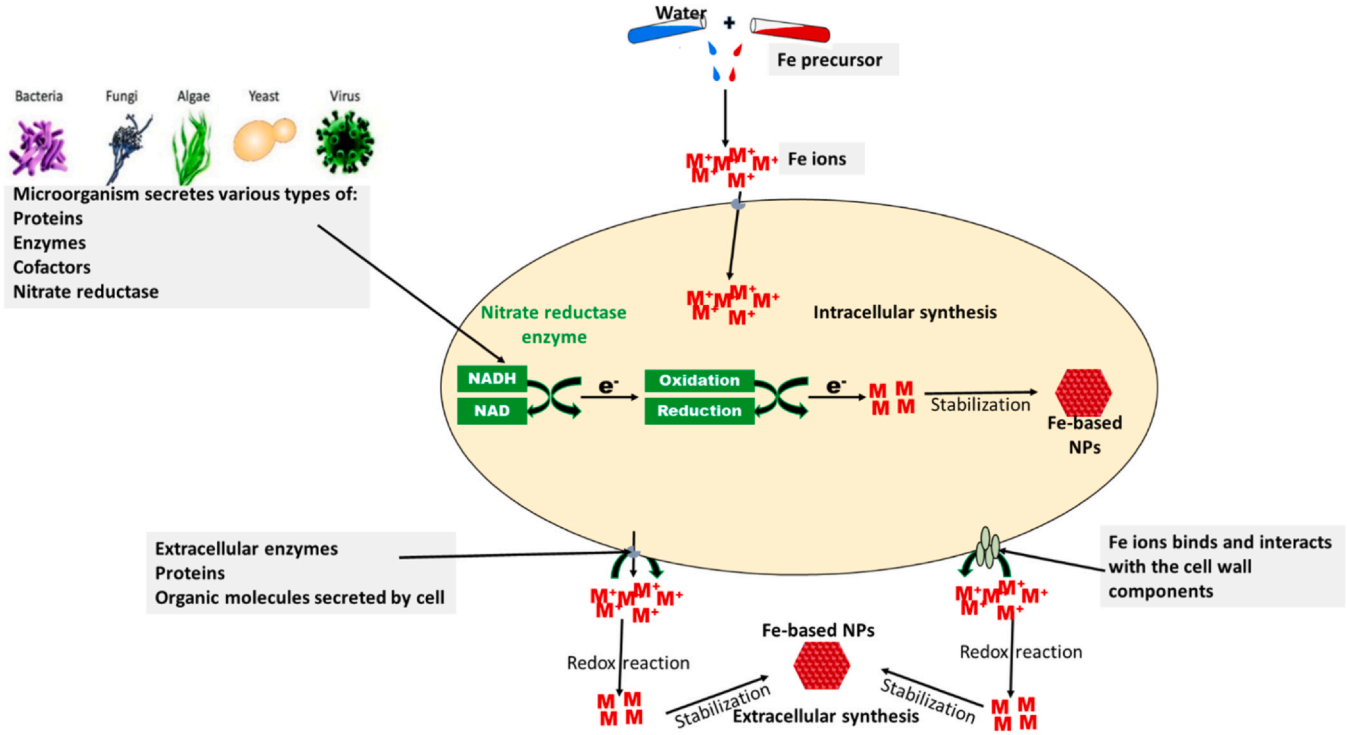

Fig. 7. Overview of mycogenic synthesis of Iron nanoparticles [53].

mycogenic entity employed, optimizing reaction conditions, controlling product quality, and ensuring [163,164]. Specifically, similar to phytogenic biosynthesis, regulated growing conditions and possible contamination concerns make scaling up for industrial purposes challenging. In addition, in the fungus-mediated production of nanoparticles, the exact mechanism behind the process remains poorly known. Therefore, more research is required to precisely define the mechanism and pinpoint the proteins and other biomolecules (enzymes) accountable for the stability and reduction of NPs[164].

8. Photocatalytic degradation performance of organochlorine and organophosphorus compounds using biogenic Iron nanoparticle and its composites

A variety of nano-engineered functional materials have been identified and reported as exceptional adsorbents and highly effective photocatalysts for the degradation of organochlorine and organophosphorus pesticides, including biogenically synthesized iron nanoparticles. The subsequent paragraphs will delve into the discussion of photocatalytic degradation efficiency of certain bio-fabricated iron-based nanoparticles. For instance, the effectiveness of Iron nanoparticles, which were synthesized using yeast extract, was examined for their capacity to degrade the organophosphorus insecticide, dichlorvos. The UV/Vis spectrum analysis of the synthesized nanoparticle revealed two distinct peaks at 216 nm and 260 nm, consistent with findings earlier reported [165–167]. Additionally, the diameter of the biologically formed FeNPs was discovered to vary between 9 and 18 nm and the TEM result displayed a uniformly distributed, spherical morphology with sizes ranging from 3–10 nm. The degradation capacity of the FeNPs' was evaluated by varying the effects of different nanoparticle concentrations, oxidants, and incubation times. This evaluation was based on a distinctive absorption peak at 208 nm, serving as the reference point. The study focused on the breakdown of dichlorvos, and this was assessed by measuring the release of phosphate ions using ammonium molybdate. The introduction of hydrogen peroxide resulted in the generation of hydroxide ions, which enhanced the degradation of dichlorvos. The most significant level of dichlorvos degradation was achieved when 2000 mg/L of FeNPs were utilized alongside 1000 µl of H_2O_2 within a 60-minute timeframe, achieving an efficiency rate exceeding 90 % [168]. In another study, irregular zero-valent iron clusters of $<$ 100 nm were biogenically synthesized by utilizing an extract of pomegranate peel as the reductant, and $FeCl_3$ as the precursor candidate to break down lindane. The decomposition process was monitored for 24 h using gas chromatography while using a FeNP concentration of 0.1 g/L. The results were remarkable, with a 99.4 % degradation of the pesticide achieved in a slightly acidic environment [169]. Lately, there have been studies where *Dalium guineense* stem bark extract has been employed to synthesize magnetic iron nanoparticles for the degradation of diverse organochlorine and organophosphorus compounds. [170]. This process utilized magnetic iron nanoparticles, which were synthesized with extracts from the stem bark of *D. guineense*, including both ethanolic and aqueous extracts, as well as iron oxide nanoparticles incorporated within carboxymethylcellulose. The spherical nanoparticles reported by Nnaji and his team were utilized to degrade a range of OCPs, including dieldrin, alpha(α)-BHC, heptachlor epoxide, beta(β)-BHC, gamma(γ)-BHC, P, P′-DDT (dichlorodiphenyltrichloroethane), delta(δ)-BHC, heptachlor, aldrin, endosulfan I, endosulfan II, endosulfan sulfate, endrin, endrin ketone, P,P′-DDD (dichlorodiphenyldichloroethane), endrin aldehyde, gamma(γ)-chlordane, P,p′-DDE (dichloro-diphenyl chloroethane), alpha(α)-chlordane, and methoxychlor. This degradation process was conducted for 180 min and resulted in an almost 100 % degradation efficiency for most of the compounds. Similarly, spherical zerovalent iron nanoparticles (Fe0) were bio-fabricated and incorporated into a biochar nanocomposite (Fe0-B_{RtP}) using waste material from *Nephelium lappaceum* fruit peel. These nanoparticles had a size range of 20–80 nm and were employed for the concurrent elimination of six specific organochlorine pesticides. As shown in Table 1, the degradation lasted for 120 mins for each pesticide achieving a remarkable efficiency of $>$ 95 %. The presence of polyphenols, including flavonoids and catechins, within the biogenic source was important to facilitate the conversion of Fe^{2+} into Fe^0.

Table 1
Summary of degradation efficiency of some biofabricated iron-based nanoparticles for organochlorine and organophosphorous pollutants.

Biosynthesized iron-based NPs	Biogenic source	Shape and size (nm)	OC and OP (Concentration (mg/L))	Light sources	pH	Dose (mg)	DE (%)	DT (min.)	References
Fe	pomegranate fruit peels	Amorphous 25.1	Lindane (50)	NS	6	100	99	1440	[169]
Fe@Mn	Blueberry pruning		chlorpyrifos-methyl (0.0005)	80 W Hg-lamp	7		85.01	5	[171]
Fe	Yeast extract	Spherical 3-10	Dichlorvos (10)	Ambient light		2000	> 90	60	[168]
Fe	*Dalium guineense* stem bark extract	Spherical	α-BHC (1.10×10^{-6})			10	-95.5	180	[170]
Fe@Mn	Brown algae		chlorpyrifos-methyl (0.0005)	80 W Hg-lamp	7		77.82	5	[171]
Fe	*Dalium guineense* stem bark extract	Spherical	β-BHC (0.98×10^{-6})			10	-40	180	[170]
Fe	*Dalium guineense* stem bark extract	Spherical	γ-BHC (1.01×10^{-6})			10	-36	180	[170]
Fe	*Dalium guineense* stem bark extract	Spherical	Heptachlor (0.97×10^{-6})			10	-17	180	[170]
Fe	*Dalium guineense* stem bark extract	Spherical	δ-BHC (0.93×10^{-6})			10	-68	180	[170]
Fe	*Dalium guineense* stem bark extract	Spherical	Aldrin (1.03×10^{-6})			10	-48	180	[170]
Fe	*Dalium guineense* stem bark extract	Spherical	Heptachlor epoxide (0.99×10^{-6})			10	-100	180	[170]
Fe	*Dalium guineense* stem bark extract	Spherical	γ-Chlordane (1.07×10^{-6})			10	-81.3	180	[170]
Fe	*Dalium guineense* stem bark extract	Spherical	α-Chlordane (0.98×10^{-6})			10	-100	180	[170]
Fe	*Dalium guineense* stem bark extract	Spherical	Endosulfan I (1.28×10^{-6})			10	-84.4	180	[170]
Fe	*Dalium guineense* stem bark extract	Spherical	P,p′-DDE (1.16×10^{-6})			10	-85.4	180	[170]
Fe	*Dalium guineense* stem bark extract	Spherical	Dieldrin (1.76×10^{-6})			10	-77.3	180	[170]
Fe	*Dalium guineense* stem bark extract	Spherical	Endrin (0.89×10^{-6})			10	-100	180	[170]
Fe	*Dalium guineense* stem bark extract	Spherical	P,P′-DDD (0.98×10^{-6})			10	-82	180	[170]
Fe	*Dalium guineense* stem bark extract	Spherical	Endosulfan II (1.21×10^{-6})			10	-100	180	[170]
Fe	*Dalium guineense* stem bark extract	Spherical	P,P′-DDT (1.37×10^{-6})			10	-100	180	[170]
Fe	*Dalium guineense* stem bark extract	Spherical	Endrin aldehyde (1.20×10^{-6})			10	-100	180	[170]
Fe	*Dalium guineense* stem bark extract	Spherical	Endosulfan sulphate (1.11×10^{-6})			10	-100	180	[170]
Fe	*Dalium guineense* stem bark extract	Spherical	Methoxychlor (0.90×10^{-6})			10	-100	180	[170]
Fe	*Dalium guineense* stem bark extract	Spherical	Endrin ketone (1.74×10^{-6})			10	-100	180	[170]
Fe@CMC	*Dalium guineense* stem bark extract	Spherical 11.95	α-BHC			10	-100	180	[170]
Fe@CMC	*Dalium guineense* stem bark extract	Spherical 11.95	β-BHC			10	-95	180	[170]
Fe@CMC	*Dalium guineense* stem bark extract	Spherical 11.95	γ-BHC			10	-91.1	180	[170]
Fe@CMC	*Dalium guineense* stem bark extract	Spherical 11.95	Heptachlor			10	-70.1	180	[170]
Fe@CMC	*Dalium guineense* stem bark extract	Spherical 11.95	δ-BHC			10	-25	180	[170]
Fe@CMC	*Dalium guineense* stem bark extract	Spherical 11.95	Aldrin			10	-86.4	180	[170]
Fe@CMC	*Dalium guineense* stem bark extract	Spherical 11.95	Heptachlor epoxide			10	-100	180	[170]
Fe@CMC	*Dalium guineense* stem bark extract	Spherical 11.95	γ-Chlordane			10	-21	180	[170]
Fe@CMC	*Dalium guineense* stem bark extract	Spherical 11.95	Endosulfan I			10	-100	180	[170]
Fe@CMC	*Dalium guineense* stem bark extract	Spherical 11.95	Dieldrin			10	-60.2	180	[170]
Fe@CMC	*Dalium guineense* stem bark extract	Spherical 11.95	Endrin			10	-28	180	[170]
Fe@CMC	*Dalium guineense* stem bark extract	Spherical 11.95	P,P′-DDD			10	-83	180	[170]
Fe@CMC	*Dalium guineense* stem bark extract	Spherical 11.95	Endosulfan II			10	-100	180	[170]
Fe@CMC	*Dalium guineense* stem bark extract	Spherical 11.95	P,P′-DDT			10	-87	180	[170]
Fe@CMC	*Dalium guineense* stem bark extract	Spherical 11.95	Endrin aldehyde			10	-93.33	180	[170]
Fe@CMC	*Dalium guineense* stem bark extract	Spherical 11.95	Endosulfan sulphate			10	-19	180	[170]
Fe@Mn	Green algae		chlorpyrifos-methyl (0.0005)	80 W Hg-lamp	7		74.89	5	[171]
Fe@CMC	*Dalium guineense* stem bark extract	Spherical 11.95	Methoxychlor			10	-100	180	[170]
Fe@CMC	*Dalium guineense* stem bark extract	Spherical 11.95	Endrin ketone			10	-100	180	[170]
Fe	*Nephelium lappaceum* fruit peel	Spherical 20-80	Endosulfan (2)		4	250	96	120	[172]
Fe	*Nephelium lappaceum* fruit peel	Spherical 20-80	Hexachlorobenzene (2)		4	250	> 96	120	[172]
Fe	*Nephelium lappaceum* fruit peel	Spherical 20-80	Heptachlor (2)		4	250	> 96	120	[172]
Fe	*Nephelium lappaceum* fruit peel	Spherical 20-80	Aldrin (2)		4	250	-99	120	[172]
Fe	green tea extract	fine globular 30-50	1,2-DCB		7.5	67.2	97.3	360	[173]
Fe	*Nephelium lappaceum* fruit peel	Spherical 20-80	o,p′-DDT (2)		4	250	-99	120	[172]

(*continued on next page*)

Table 1 (*continued*)

Biosynthesized iron-based NPs	Biogenic source	Shape and size (nm)	OC and OP (Concentration (mg/L))	Light sources	pH	Dose (mg)	DE (%)	DT (min.)	References
Fe@Mn	Black tea		chlorpyrifos-methyl (0.0005)	80 W Hg-lamp	7		77.23	5	[171]
Fe	*Nephelium lappaceum* fruit peel	Spherical 20-80	p,p′-DDT (2)		4	250	-99	120	[172]

carboxymethyl cellulose = CMC, AC = activated carbon, BC = biochar, HCF = hexacyanoferrate, reduced graphene oxide = rGO, BSNPs = Biosynthesized nanoparticles, DE = Degradation efficiency, DT = Degradation time, OP = Organochlorine, OP = Organophosphorus/Organophosphate, δ-BHC = delta Benzene hexachloride, β-BHC = beta Benzene hexachloride, gamma = γ, alpha = α, P,p′-DDE = dichloro-diphenyl chloroethane, P,P′-DDD = dichlorodiphenyldichloroethane, P,P′-DDT = dichlorodiphenyltrichloroethane, α-BHC = alpha Benzene hexachloride, 2,4-D = 2,4-dichlorophenoxy acetic acid, 2,4-DP = 2-(2,4-dichlorophenoxy)-propionic acid, γ-BHC = gamma Benzene hexachloride.

9. Photocatalytic degradation performance of organochlorine and organophosphorus compounds using biogenic Iron oxide nanoparticle and its composites

Without gainsaying, aside from bio-fabricated iron-based NPs reported in the forgoing section, Iron oxide-based nanoparticles, particularly those biogenically synthesized, have emerged as a promising material for efficiently breaking down organochlorine and organophosphorus compounds. The results of some of these biogenic iron oxide nanoparticles are summarized in the succeeding paragraphs and Table 2.

For instance, Wend and his team [174] reported the biogenic synthesis of magnetite Fe_3O_4 nanoparticles for the removal of doxorubicin hydrochloride which is an organochlorine compound. Spherical nanoparticles with an average size of 10–30 nm were prepared using *Euphorbia cochinchinensis* extract and their results were similar to what was obtained by Prasad and his colleagues [175]. In comparison to the commercial Fe_3O_4 nanoparticles, which were used at a concentration of only 20 mg/L, the biogenically synthesized nanoparticles exhibited remarkable removal efficiency. After a 48-hour duration, they achieved an impressive removal efficiency of 80.2 % for the substance, while the commercial Fe_3O_4 nanoparticles only managed to degrade 23.5 % of DOX. The exceptional degradation capability of these nanoparticles is credited to their substantial specific surface area (measuring 79.9 m^2/g), diminutive size (ranging from 10 to 30 nm), and the existence of phenolics and flavonoids in the leaf extract. The pH dependency of DOX removal is evident, with the removal efficiency of DOX showing a gradual increase from 57.2 % to 87.9 % as the pH of the solution shifted from 3 to 7. Beyond this range, specifically in the pH range of 7 to 9, no additional improvement in removal efficiency was observed. This suggests that hydrogen ions in the adsorption process compete with DOX, particularly at lower pH levels. When the pH level rose and approached saturation, the process stabilized and the degradation behavior was limited[176,177]. Additionally, the effective degradation of DOX on the surface of Fe_3O_4 was verified by the presence of functional groups from DOX, as indicated by fresh bands at 1282 and 990 cm^{-1} in the stretching vibration of C-O-C. Fe_3O_4 nanoparticles synthesized through a green approach exhibit remarkable magnetic properties. After their use in DOX removal, they demonstrated high recyclability and regenerative capabilities. Also, an analysis of the magnetic properties using a SQUID magnetometer revealed that these nanoparticles are ferromagnetic, with a saturation magnetization value of 359 emu/g. [178]. In 2018 El-said and his colleagues synthesized a novel magnetite MSNPs/Fe_3O_4 nanocomposites by employing extracts from green tea as capping and reducing agents. After 420 mins, the quasi-spherical nanocomposite of diameter 30 nm was used to degrade an organochlorine pesticide known as lindane with more than 99 % efficiency [179]. The remarkable use of the nanocomposite to be able to capture lindane is due to an increase in the contact time, a slightly acidic medium to neutral pH as it was revealed that there is no removal of lindane in the alkaline medium unlike the removal of DOX, as well as the magnetic feature which is important when separating lindane from waste water with the use of an external magnetic field [174]. The absorption spectrum of lindane at a neutral pH showed a peak at 270 nm. However, as the pH increased, the peak shifted to longer wavelengths, reaching 286 nm. This shift indicates a de-chlorination of lindane, suggesting that lindane is unstable in an alkaline medium. Additionally, the confirmation of lindane removal involved examining the FTIR spectra for changes in functional groups. The emergence of a novel peak in the MSNPs/Fe_3O_4 nanocomposite bound to the pesticide, shifting away from the typical C-Cl functionality at 1385 cm^{-1}, served as evidence of adsorption. Additionally, the magnetic characteristics of the manufactured nanoparticles were assessed through VSM measurements conducted at room temperature.

In another investigation, Pushkar and Sevak focused on the removal of the organochlorine pesticide DDT. They employed biogenically

Table 2
Summary of degradation efficiency of some bio-fabricated iron oxide-based nanoparticles for organochlorine and organophosphorus pollutants.

Biosynthesized iron oxide-based NPs	Biogenic source	Shape and size (nm)	OC and OP (Concentration (mg/L))	Light sources	pH	Dose (mg)	DE (%)	DT (mins)	References
BC@$NiFe_2O_4$	*Murraya koenegii* leaves	Spherical	Endosulfan (50)	sunlight	3	10	92	30	[186]
Citrus limetta BC@ Fe_2O_3	green tea extract	spherical 8	Endosulfan (50)	sunlight	3	25	94	300	[183]
$CdMgFe_2O_4$ @TiO_2	Guar gum	Spherical 18–34	DDE (20)	sunlight	7	20	89	210	[182]
BC@$NiFe_2O_4$	*Murraya koenegii* leaves	Spherical	Atrazine (50)	sunlight	3	10	98	30	[186]
BC@ β-FeOOH	*Citrus limetta* waste peels	Spherical	Endosulfan (20)	Sunlight	4	25	80	> 120	[187]
BC@ α-FeOOH	*Citrus limetta* waste peels	Rod	Endosulfan (20)	LED bulb	4	25	25-35	> 120	[187]
Fe_3O_4	*euphorbia cochinchinensis* extract	Spherical 10–30	Doxorubicin hydrochloride (20)		6	20	80.2	48 *	[174]
$NiFe_2O_4$	*Murraya koenegii* leaves	Spherical	Atrazine (50)	sunlight	3	10	~40	30	[186]
Fe_2O_3	green tea extract	spherical 8	Endosulfan (50)	sunlight	3	25	< 50	300	[183]
SiO_2 @ Fe_3O_4	green tea leaf	quasi-spherical	Lindane (40)			90	> 99	420	[179]
BC@ α-FeOOH	*Citrus limetta* waste peels	rod	Endosulfan (20)	Sunlight	4	25	98	> 120	[187]
$CuFe_2O_4$	Arabic Gum-grafted-polyamidoxime	*37*	Chlorpyrifos (300)		6	5	> 90	15	[181]
$NiFe_2O_4$	*Murraya koenegii* leaves	Spherical	Endosulfan (50)	sunlight	3	10	> 35	30	[186]
$CdMgFe_2O_4$ @TiO_2	Guar gum	Spherical 18–34	Endosulfan (20)	sunlight	7	20	95	210	[182]
BC@ α-FeOOH	*Citrus limetta* waste peels	Rod	DDD (20)	Sunlight	4	25	92	> 120	[187]
Fe_3O_4	Neem leaves extract	Spherical 21.03-80	DDT (50)	-	3	-	90.2	120	[180]
Citrus limetta BC@ Fe_2O_3	green tea extract	spherical 8	Ethion (50)	sunlight	3	25	91	300	[183]
$NiFe_2O_4$	*Murraya koenegii* leaves	Spherical	Atrazine (50)	artificial bulb	3	10	> 30	30	[186]
BC@ β-FeOOH	*Citrus limetta* waste peels	Spherical	DDD (20)	sunlight	4	25	78	> 120	[187]

synthesized Fe oxide nanoparticles, which were created using Neem leaf extract as both a reducing and stabilizing agent. The formation of Fe_3O_4 nanoparticles was verified by a noticeable change in the color of the aqueous solution of the iron precursor, ferric chloride, from yellowish to a deep black hue. The presence of a distinct peak at 304 nm confirmed the generation of Iron oxide nanoparticles, and the presence of a narrow peak at 304 nm indicated their mono-dispersity. Spherically shaped nanoparticles were formed with an average size of 80 nm, although their surface was not uniform [180]. As reported in previous studies [174,179], varying the pH is an important parameter for achieving an optimum result (removal of pollutant steadily decreases as the pH of the solution is increased), thus 88–92 % of DDT was degraded with a maximum concentration of 500 ppm of DDT by the bio-fabricated green Fe_3O_4 NPs at a pH 3 (a strongly acidic medium). Other parameters such as time of contact and DDT concentration were also varied and it was revealed that the longer the contact time the higher the removal rate but the higher the concentration the lower the removal of the pollutant [180]. In recent times, novel Iron oxide nanoparticles have been synthesized to remove stubborn pollutants achieving an outstanding efficiency within a relatively short period. A novel superparamagnetic adsorbent was developed by modifying a polysaccharide known as Gum Arabic with polyamidoxime to facilitate the degradation of the chlorpyrifos pesticide from contaminated water. The process involved the creation of a biosorbent hydrogel nanocomposite through several steps. Initially, $CuFe_2O_4$ MNPs were synthesized using the co-precipitation method by first using free radical polymerization to graft the acrylonitrile (AN) monomer onto the Gum Arabic (AG) chain followed by modifying AG-g-PAN/$CuFe_2O_4$ by using hydroxylamine hydrochloride and NaOH solution. Within 15 mins of exposure of the nanocomposite to the chlorpyrifos pesticide, about 99 % of it had been removed at a pH of 6 with just 0.005 mg of the adsorbent. Efficient removal of the organophosphorus pesticide was attributed to the presence of numerous reactive functional groups or adsorption sites, including amidoxime, hydroxyl, amide, and carboxyl groups. These groups, in conjunction with a three-dimensional network, interacted with chlorpyrifos through mechanisms like electrostatic interaction and hydrogen bonding. The experimental adsorption kinetics fit well with the pseudo-second-order model, providing an overall confirmation of the high efficiency of the prepared bio-adsorbent. [181]. Going forward, guar gum was incorporated in $CdMgFe_2O_4$ @TiO_2 nanocomposite to optimize and improve its efficiency in degrading hazardous pesticides [182] forming distorted cubic and spherically shaped nanoparticles and nanocomposites. Meanwhile, guar gum (GG) displayed an irregular flake-like morphology. However, when GG was incorporated into a polymeric matrix, its morphology transformed into a sheet-like structure. The shape obtained in the photodegradation experiment is accordant with the one reported by Rani et al., where combination biochar (BC) was prepared using waste peels of *Citrus limetta* embedded with green synthesized Fe_2O_3 nanoparticle by using green tea extract [183] whereas there was a low degradation efficiency (< 50 %) achieved when Fe_2O_3 nanoparticles confirming the effectiveness of doping the Iron oxide nanoparticles with other materials such as GG which act both as capping and stabilizing agents, effectively encapsulating the nanomaterial. This encapsulation results in remarkable light absorption properties across the entire spectrum owing to the strong H-bonding and cross-linking capabilities of the -OH groups [184,185]. About 20 mg of the prepared 100 nm GG-$CdMgFe_2O_4$ @TiO_2 was used to degrade 94 % Endosulfan (ES) and 88 % DDE at neutral pH under sunlight after 180 mins [182] by varying the concentrations of pesticides (ranging from 20 to 40 mg/L), the amount of nano-catalyst (between 15 to 35 mg), and pH levels (from 3 to 11). The findings indicated that as the concentrations of ES and DDE surges, the degradation output decreased for all nano-catalyst quantities. Also, Rani and his team compared the use of green tea extract to synthesize Fe_2O_3 nanoparticle and BC synthesized by using waste peels of *Citrus limetta* to comparatively degrade two pesticides, Endosulfan and Ethion. Both

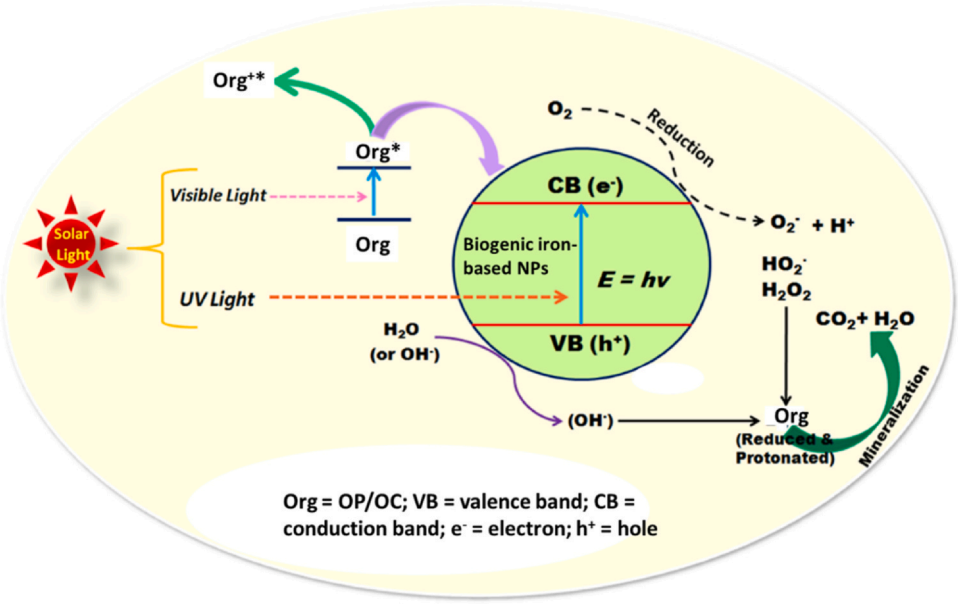

Fig. 8. General mechanism of photodegradation of OP/OC using bio-fabricated iron-based nanoparticles as the catalysts[190].

nanoparticles yielded an 8 nm spherical catalyst but a higher degradation efficiency was achieved for *Citrus limetta* BC@ Fe_2O_3 (94 % ES; 91 % ET) in contrast with Fe_2O_3 (< 50 % ES; < 40 % ET) after 300 mins under natural sunlight [183]. It was concluded that hybrid BC@Fe_2O_3 showed better photocatalytic effectiveness and averted the ability of generated e^-/h^+ duos to recombine when exposed to visible light.

10. Photodegradation mechanism of organochlorine/ organophosphorus compounds

Photocatalysts are responsible for an economically viable degradation of organic pollutants such as OP/OC in the presence of sunlight or Uv-radiation[188]. Biogenic iron (Fe)–based nanoparticles have shown promise in facilitating the degradation of OP and OC via a process known as photocatalysis[189]. Generally, the mechanism of photodegradation of OP/OC using biogenic metal-based nanoparticles as catalysts including FeNPs, involves several steps such as; reactive oxygen species (ROS) generation, OP/OC adsorption on the surface of catalysts, degradation of adsorbed OP/OC by the ROS, and mineralization of degradative products to simple, environmental benign molecules like carbon dioxide, water, or inorganic ions (Fig. 8)[190].

The general mechanism of photocatalytic degradation of OP/OC using iron nanoparticles (FeNPs) may be represented by the following reactions in Eqs. 1–8 [190]:

$$FeNPs + h\nu \rightarrow h^+ + e- \text{ (photogeneration of excitons)} \quad (1)$$

$$H_2O + h^+(VB) \rightarrow \bullet OH^+ H^+ \quad (2)$$

$$OH^- + h^+ \rightarrow \bullet OH \quad (3)$$

$$e^-(CB) + O^2 \rightarrow \bullet O_2^- \quad (4)$$

$$\bullet O_2^- + H^+ \rightarrow \bullet OOH/H_2O_2 \quad (5)$$

$$H_2O_2 \rightarrow \bullet OH + \bullet OH \quad (6)$$

$$Org + h\nu \rightarrow Org^{*}\cdot \quad (7)$$

$$Org^* + O_2 \text{ or } {}^{\bullet}OH \text{ or } {}^{\bullet}O_2^- \rightarrow \text{(unstable intermediate)} \rightarrow CO_2 + H_2O \quad (8)$$

Org = OP/OC; VB = valence band; CB = conduction band

The generation of ROS begins with an initiation step, where FeNPs photocatalysts are exposed to ultraviolet radiation or sunlight, subsequently absorbing the photon energy[191]. The initiation mechanism started by transferring electron (e^-) from the photocatalyst valence band (VB) into its conduction band (CB) provided the light energy is > the photocatalyst band gap[191], leading to holes (h^+) creation, which in turn produce e^-/h^+ pairs within the excited photocatalyst as depicted in Eq. (1) [190,191]. The reaction between the holes generated and the H_2O molecule forms hydroxyl radical (•OH) and hydroxonium ions (H^+) as presented in Eq. (2). There is also a possibility of interaction between the holes and the catalyst surface adsorbed hydroxyl anion to generate hydroxyl radical shown in Eq. (3). Then, the excited e^- in the CB reacts with the molecular oxygen (O_2) and the hydronium ions present in solutions to generate superoxide radical anion and hydrogen peroxide, further dissociation of these ROS in the presence of oxygen, generates hydroxyl ions, as depicted in Eqs. (4–6). Moreover, the generated ROS and the holes could interact efficiently with organic pollutants such as OP/OC compounds. Finally, the captured electron by the molecular oxygen migrated into the VB and was then trapped by OH^- or H_2O species previously adsorbed on the surface of the catalyst to $^{\bullet}OH$, which subsequently facilitated oxidative cleavage of the organic pollutants to smaller unstable intermediate, and finally into CO_2 and H_2O as represented in Eqs. (7 and 8) [190–192].

Generally, the mechanism by which organic contaminants including OP/OC are degraded by photocatalysis follows either a direct or indirect degradation mechanism pathway.

10.1. Direct degradation pathway

Degradation of organic pollutants occurs in the presence of easily absorbed visible light radiation. The excitation of electrons occurs from the organic pollutant singlet ground state into the triplet excited state under visible light with > 400 nm wavelength. Further migration of this triplet excited state electron from the organic pollutant into the FeNPs CB generates a partially oxidized radical cation analog of the pollutant. The dissolved molecular oxygen in the solution then trapped the electron from the FeNPs CB to form superoxide radical anions (O_2^-), which further transformed into hydroxyl radical ($OH^{\bullet}$). Finally, the oxidative degradation of the pollutant is facilitated by the generated $OH^{\bullet}$ [193].

10.2. Indirect degradation pathway

This involved the photoexcitation of an electron from the lowest occupied molecular orbital (HOMO), i.e. the VB of the photocatalyst to generate a hole (h^+) into the highest unoccupied molecular orbital (LUMO), i.e. CB containing unpaired electron (e^-). The photogenerated holes then interact with the water to form the hydroxyl radical ($OH^•$). Moreover, a non-selective interaction between the $OH^•$ and previously adsorbed organic pollutants on the surface of the catalyst enhances the degradation or mineralization of the pollutant depending on the structural morphology and stability of the pollutant. To maintain the electron neutrality with the photocatalyst, molecular oxygen in solution trapped the electron in the catalyst CB to produce O_2^-, which not only prevents electron-hole aggregation but also participates in further oxidation of the OP/OC. The protonation of O_2^- forms H_2O_2, which then decomposes into highly unstable $OH^•$ [193].

11. Effect of operating parameters

11.1. Effect of radical scavengers

A scavenger experiment involving trapping or quenching free radicals including h^+ and $e-$ is employed to identify the reactive species (RS) participating in pollutant degradation and measure and evaluate the quantity of biogenic nanocatalyst inhibitor/antagonist present during a catalysis operation. Scavengers hinder or obstruct a catalyst's function, which lessens the catalyst's capacity to facilitate the intended chemical reaction[186,194].

Notably, only a few studies have explored the impact of radical scavengers on the photocatalytic degradation of organochlorine and organophosphorus contaminants using biogenic iron-base nanoparticles. For instance, to explore the role of various reactive radical species in the photocatalytic degradation of Endosulfan and Atrazine using biogenic BC@$NiFe_2O_4$, *tert*-butyl alcohol (TBA), para-benzoquinone (para-BQ), ethylenediaminetetraacetic acid disodium salt (Na_2EDTA) were employed as $^•OH$, $•O_2^-$ and h^+ radical scavengers [186]. For this, 5 mg/L of Endosulfan, 15 mg of biogenic BC@$NiFe_2O_4$ at acidic pH, and 2 mL of quenchers were exposed to sunlight for about half an hour and the same procedure was carried out in the case of Atrazine. In addition, an exact duplicate sample devoid of quencher was generated to serve as a comparative study. The result revealed that the least photocatalytic degradation was seen in TBA, and then para-BQ as shown in the degradation efficiency plot of both contaminants displayed in Fig. 9. Interestingly, the highest photocatalytic degradation efficiency was observed in the sample without the scavengers. Nevertheless, the Na_2EDTA-containing test also exhibited effectual Endosulfan and Atrazine photocatalytic degradation. These radical scavenging findings show that h^+ and $•O_2-$ play supportive roles in the photocatalytic degradation of both Endosulfan and Atrazine, while the •OH plays a prominent role as the active species i.e. •OH is largely in control of the photocatalytic degradation of both Endosulfan and Atrazine using biosynthesized BC@$NiFe_2O_4$[186]. Similarly, in another study[182] for the photocatalytic degradation of DDE and Endosulfan using biosynthesized $CdMgFe_2O_4$ @TiO_2, isopropyl alcohol (IPA), BQ, triethanolamine (TA) were employed as $^•OH$, $•O_2^-$ and h^+ radical scavengers. For this, 20 mg/L of DDE, 20 mg of biogenic $CdMgFe_2O_4$ @TiO_2 at pH 7, and 2 mL of quenchers were exposed to sunlight for about 210 min and the same procedure was carried out in the case of Endosulfan. The result revealed that when the respective radical quencher was added, the degradation percentages of both DDE and Endosulfan decreased with the inhibitory effect of TA coming to the fore, followed by IPA and BQ. These radical scavenging results demonstrate that h^+ and $•O_2-$ play minor roles in the photocatalytic degradation of both Endosulfan and DDE, while •OH largely controls the photocatalytic degradation operation i.e there were more •OH radicals than other reactive species[182]. Also, Rani's research group [187] did not differ in their report. In this report, when EtOH, BQ, and TA were employed to study the effect of radical scavengers on the photocatalytic degradation of Endosulfan and DDD using biosynthesized BC@ α-FeOOH and BC@ β-FeOOH, it was discovered that •OH radical played the main function in the photocatalytic degradation process of the pollutants compared to other reactive radical species like h^+ and $•O_2-$ [187].

In summary, there is an inverse relationship between radical scavengers and photocatalytic degradation efficiency. Notably, the degradation efficiency is often reduced by the presence of radical scavengers that trap electrons. By absorbing electrons or reactive radicals created during the photocatalytic process, these scavengers can prevent the development of reactive species, which are essential for the attack and breakdown of the pollutants. Additionally, from our own perspective, the presence of a plethora of phytochemicals containing OH and other oxygenated functional groups in the biogenic entities [87,195] employed for the biosynthesis of Fe-based nanomaterials probably contributes to the dominance of OH radical role in the

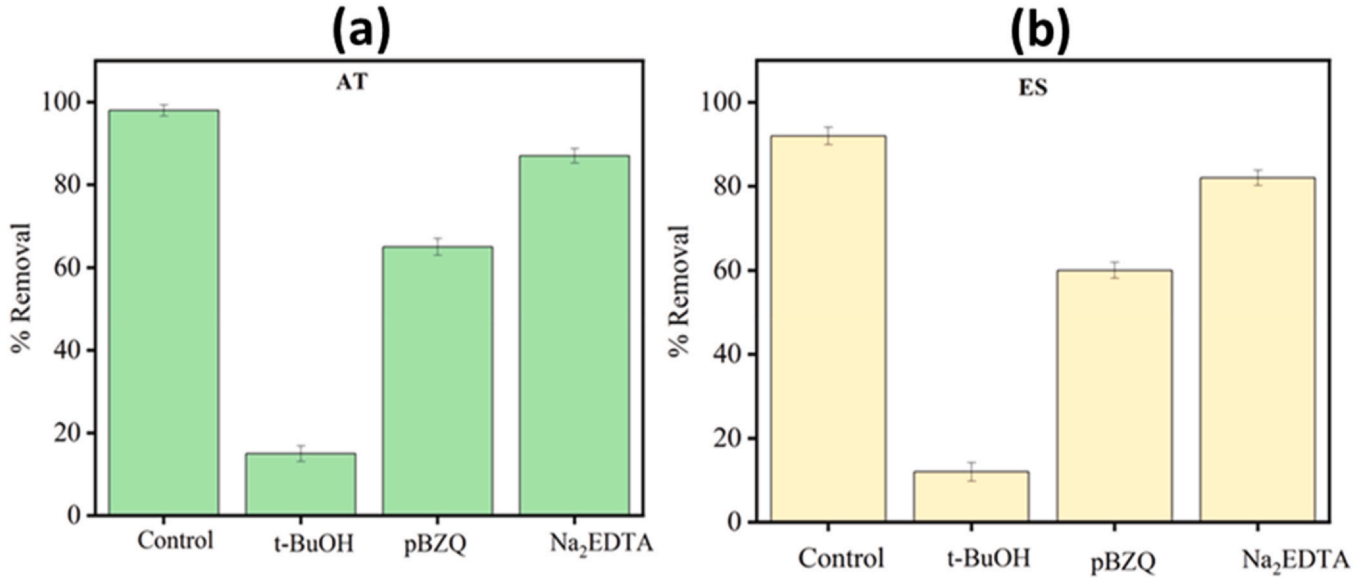

Fig. 9. Effect of different free radical scavengers on photocatalytic degradation of (a) Atrazine and (b) Endosulfan using biosynthesized BC@$NiFe_2O_4$[186].

photocatalytic degradation of organochlorine and organophosphorus agro-pollutants.

11.2. Effect of pH

pH significantly influences various environmental processes, particularly in the realm of environmental remediation. The initial pH of the solution is critical for the FeNP performance as it can affect both the degree of ionization of the dye pollutant and the surface charge, functional groups, and properties of the photocatalyst [196,197] Weng et al [174] emphasize pH substantial impact on the photocatalytic degradation of organochlorine pollutants using Fe_3O_4 photocatalyst synthesized with *Euphorbia cochinchinensis* extract. This influence stems from alterations to the catalyst's surface charge, reactant degradation, and the generation of ROS, notably hydroxyl radicals (OH•), which enhance pollutant degradation, especially in acidic conditions. Batool et al [172] stress the significance of regulating initial pH levels, significantly impacting degradation efficiency. This underscores the pivotal role of pH control, especially in dichlorination processes involving nanocomposites like Fe0-BRtP and chemically synthesized Fe0-BChe. In this investigation, as the pH level ranged from 5 to 12, the elimination of pesticides using Fe0-BRtP and Fe0-BChe declined, and the most efficient degradation was observed at pH 4 with a degradation percentage of about 80 %. Beyond a pH of 4, secondary reductants developed on the iron (Fe) surface, leading to a decrease in the efficiency of degradation. Under mildly acidic conditions (pH $<$ 5), these reductants were eradicated, facilitating iron's engagement in the dichlorination process. However, in strongly acidic environments, an excessive presence of H^+ ions resulted in damage to the carbon and Fe0 oxidation, consequently reducing the capacity for Fe pollutant degradation using Nephelium lappaceum fruit peel. Consequently, a pH of 4 is identified as the optimal pH level for achieving maximum dichlorination of organochlorine pollutants within a pesticide-Fe0-BRtP-water system [172]. El-Said research group[179] delves into the interplay between pH and temperature, revealing their crucial roles in efficiently removing nanocomposites during lindane pesticide degradation. pH influences the surface charge and ionization of the pesticide, while temperature affects the kinetics and thermodynamics of the degradation process. Another team[181] points out the substantial impact of varying pH levels on the degradation process, with alterations in surface charge affecting the composite's affinity for chlorpyrifos. Keshu and his team[182] establish a connection between pH and the degradation of Endosulfan (ES) and DDE under neutral pH conditions. This indicates that variations in pH alter surface charge and chemical reactivity, influencing both degradation and the photocatalytic degradation of pesticides. Pushkar's team [180] emphasizes pH's role in DDT degradation, demonstrating that maximum degradation occurs at pH 3[182]. This underscores the crucial nature of pH control in achieving efficient pollutant degradation. The pH significantly influences the degradation of DDT on Fe_3O_4 nanoparticles, with maximum degradation (90 %) occurring at pH 3 due to favorable electrostatic attraction, while degradation gradually decreases as the pH increases, attributed to the changing surface charge of the adsorbent and electrostatic repulsion caused by hydroxyl ions [182]. Lastly, [183] discovered that their nanohybrid was effective under acidic conditions, highlighting the significance of pH control in ensuring efficient pesticide breakdown during photocatalysis. In different contexts, [168–170,198] may not explicitly mention pH's role in their studies, but they acknowledge its importance in catalytic reactions, affecting surface charge and reactant ionization.

11.3. Effect of temperature

Temperature significantly influences reaction kinetics, that is the mobility of pollutant ions [199]. Higher temperatures generally accelerate reactions by increasing kinetic energy, facilitating reactant diffusion and energy availability. However, maintaining the optimal temperature range is crucial to prevent catalyst or reactant thermal decomposition[174]. Batool's team[172] discovered that elevating the temperature from 25 °C to 45 °C had a beneficial impact on eliminating Organochlorine and Organophosphate Pollutants (OCPs) using Fe0-BRtP, Fe0-BChe, and Nephelium lappaceum fruit peel. Initially, at 25 °C, Fe0-BRtP removed approximately 86–91 % of OCPs in 120 min, while Fe0-BChe removed 76–86 % in 150 min. Nevertheless, with the temperature increase to 45 °C, during the same periods, there was a significant enhancement in degradation rates, reaching 96–99 % for Fe0-BRtP and 83–91 % for Fe0-BChe. The rapid degradation of OCPs highlights the influence of temperature on these nanocomposites' efficiency. Kinetic models indicate that pseudo-second-order degradation and pseudo-first-order reduction mechanisms primarily govern degradation[172]. El-Said et al. investigate the interplay of pH and temperature, emphasizing their roles in efficiently removing lindane pesticides. pH variations affect the composite's surface charge and the pesticide's ionization, while temperature influences the kinetics and thermodynamics of the degradation process[179]. While [168–170,180,198] does not detail temperature's specific effects, it is important to note that temperature significantly impacts catalytic reaction rates. Higher temperatures enhance reaction kinetics due to increased kinetic energy but must be carefully controlled to prevent thermal degradation. Temperature remains a crucial factor in reaction kinetics, with the rate of pollutant degradation varying significantly based on temperature. Optimal temperature ranges are essential for maintaining efficiency. Temperature's role in reaction kinetics, especially in nanoparticle-based degradation processes, should not be underestimated. In the context of photocatalysis, temperature's influence on reaction kinetics is a critical consideration.

11.4. Effect of residence time

Time is a fundamental parameter influencing pollutant degradation in various studies. Longer reaction or contact times provide increased opportunities for interactions between the catalyst, adsorbent, or nanomaterial and pollutants, resulting in more efficient pollutant degradation. However, this parameter must be meticulously optimized to ensure efficient degradation. In another context, Hassanzadeh-Afruzi et al. [181] found that the contact time between the photocatalyst and the chlorpyrifos solution plays a vital role in the degradation processes. Longer contact times generally result in more efficient degradation. Moreover, [182] suggested that the duration of exposure to sunlight or reaction time is a crucial operating parameter for the degradation of Endosulfan (ES) and DDE. Longer exposure times typically lead to more efficient degradation of pesticides. In another study[168], the effects of incubation time on the degradation activity of FeNPs were highlighted. Longer incubation times likely provide more opportunities for molecules to interact with the FeNPs, resulting in enhanced degradation. Additionally, Ningthoujam's team[169] indicated that 0.1 g/L of FeNPs degraded approximately 99 % of lindane within 24 h, emphasizing the essential role of reaction time in achieving efficient pollutant degradation. Paknikar et al[198] emphasized the importance of understanding the time required for degradation in practical applications, as their nanoparticles efficiently degraded lindane over 8 h. In yet another context, Rani et al. demonstrated the critical role of contact or reaction time in achieving effective pesticide degradation, as the process required a specific duration for successful degradation[183]. Finally, Pushkar et al. highlighted that the contact or incubation time is a key parameter for optimizing the degradation process[180]. The study found that the maximum degradation equilibrium for DDT was reached after two hours, after which DDT began to desorb from the nanoparticles The impact of time was examined to establish the equilibrium period for degradation, with the findings indicating rapid DDT degradation on iron oxide nanoparticles within 2 h, achieving 60–85 % degradation due to the abundant active binding sites and high surface[180].

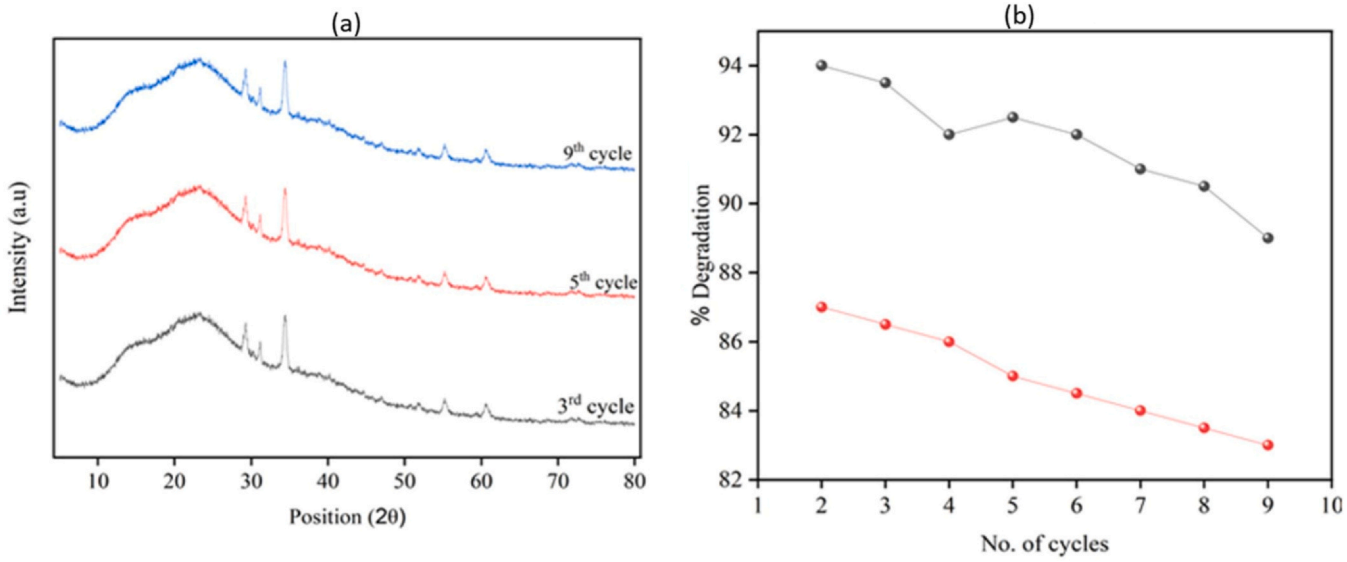

Fig. 10. (a) PXRD analysis of biogenic GG-$CdMgFe_2O_4$ @TiO_2 stability study (b) Recyclability study of biogenic GG-$CdMgFe_2O_4$ @TiO_2 for photocatalytic degradation of ES and DDE [182].

11.5. Effect of nano-catalyst dose

The quantity of nanoparticles or catalysts plays a critical role in various studies. Higher doses provide more active sites for reactions, but balance is essential to avoid issues like increased scattering[174]. Efficient degradation and dechlorination hinge on the successful dispersion of Fe0 nanoparticles on biochar surfaces. For example, Batool's team [172] found that green-synthesized Fe0-BRtP exhibited consistent reactivity, highlighting stability. The research revealed that as the adsorbent dosage increased, the degradation of OCPs also increased. This relationship is due to the expansion of the degradation surface area and the greater availability of active sites. The highest degradation rates, at 86–91 % and 76–86 %, were obtained when 0.45 g L1 dosages of Fe0-BRtP and Fe0-BChe were used. Notably, once this 0.45 g L1 dosage was reached, the degradation percentage remained steady. Using mesoporous silica nanoparticles with iron oxide in nanocomposites, as shown by El-Said's research team[179], emphasizes the importance of nanoparticle characteristics for creating a high surface area for interaction with chlorinated compounds. Another research group[181] discussed the influence of biosorbent dosage on degradation capacity for $CuFe_2O_4$ using Arabic Gum-grafted-polyamidoxime, emphasizing the provision of more binding sites with higher doses. In the case of Keshu et al., the nanocomposite dose was optimized for efficient pesticide degradation[182]. Nnaji et al[170] also stressed that the concentration of nanoparticles significantly affects the rate and extent of removal. Similarly, Pushkar et al. underlined the essential role of Fe-oxide nanoparticle concentration in DDT degradation[180]. In another research [183], a catalytic dose of 25 mg was found effective in pesticide degradation. The amount of the catalyst significantly impacts the rate and extent of removal.

11.6. Effect of initial OC and OP concentration

By and large, researchers observed that higher pollutant concentrations diminished the degradation output due to the oversaturation of the employed nanomaterial. Higher concentrations may require longer reaction times or increased catalyst doses. However, excessively high concentrations can hinder reaction kinetics due to limited active sites[174]. High degradation percentages suggest the efficiency of nanocomposites in handling elevated initial pollutant concentrations, such as OCPs[172]. This indicates their effectiveness across various pollution levels. El-Said et al., 2018 demonstrated a high sorption capacity (around 99 %) of mesoporous silica nanoparticles/iron oxide nanocomposites for lindane molecules, implying effectiveness even at elevated initial SiO_2, and Fe_3O_4 pollutant concentrations [179]. Regarding the study by[181], the initial concentration of chlorpyrifos is crucial. Higher initial concentrations may require more adsorbent or extended contact times for efficient degradation. Mehrotra et al. emphasize the importance of the initial concentration of dichlorvos. Higher concentrations may necessitate longer reaction times or increased catalyst doses for efficient degradation[168]. In a study by another group of researchers[180] the impact of Fe_3O_4 pollutant concentration on degradation efficiency was investigated using DDT concentrations up to 500 ppm. Higher initial concentrations may necessitate longer contact times or increased nanoparticle doses for effective degradation. The study of DDT degradation by Fe3O4 nanoparticles, covering concentrations from 50 ppm to 1000 ppm, showed that degradation efficiency increases up to 500 ppm but declines beyond this point. This suggests that at lower concentrations, a larger proportion of available degradation sites on the adsorbent are utilized per mole of solute, leading to enhanced degradation, a phenomenon consistent with prior research. Rani et al. in 2023 worked with a pollutant concentration of 50 mg/L, underscoring the significance of Citrus limetta and Fe_2O_3 pollutant concentration in influencing the efficiency of photocatalytic processes[183]. Higher initial concentrations may necessitate longer reaction times or increased catalyst doses for effective degradation. Understanding initial pollutant concentrations is crucial in wastewater studies, as higher concentrations may require longer contact times or increased nanoparticle doses for efficient degradation.

11.7. Recyclability and regenerability of biogenic Fe-based photocatalyst

Catalyst's recyclability is an important factor to be considered in catalysis experimental design, especially in the photocatalytic degradation of organic pollutants. The overall catalytic activity, efficiency, robustness, and stability of biogenic-based FeNP catalysts can be evaluated via reusability analysis[200]. Moreover, catalysts recyclability determines the economic aspects of the catalyst, the higher the number of times a catalyst can be reused or regenerated without losing its catalytic properties, the more economical it is. The reusability of biogenic-based photocatalysts is usually evaluated through a series of cyclic experiments and determines the cycle at which the catalysts' degradation efficiency is identified[200]. For example, in a particular study[182], the recyclability and stability of biogenic GG-$CdMgFe_2O_4$

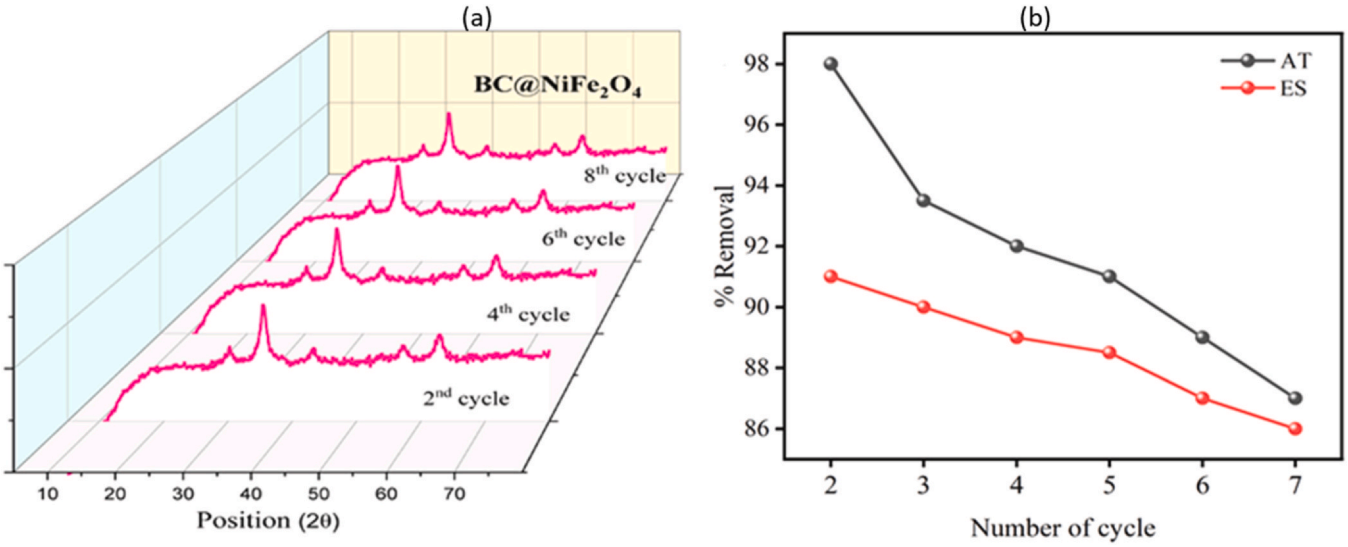

Fig. 11. (a) PXRD analysis of biogenic BC@$NiFe_2O_4$ stability study and (b) Recyclability study of biogenic BC@$NiFe_2O_4$ for photocatalytic degradation of Atrazine (AT) and Endosulfan (ES) [186].

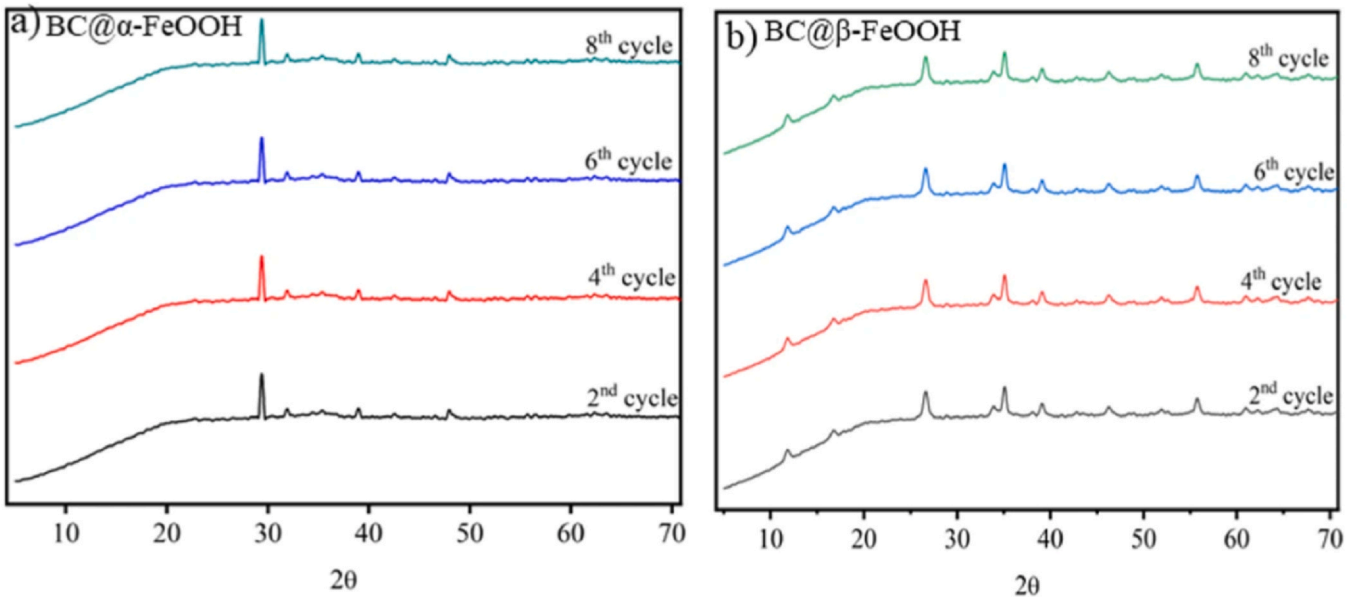

Fig. 12. PXRD spectral of spent biogenic (**a)** BC@ α-FeOOH and (**b)** BC@ β-FeOOH for photocatalytic degradation of Endosulfan and DDD[187].

@TiO_2 were examined for the photocatalytic degradation of ES and DDE. Following each round, the biogenic NP was centrifuged to remove the photocatalyst from the reaction mixture. It was then repeatedly cleaned with distilled H_2O and acetone and heated to 60 °C for six hours to test the catalyst's reusability. Successful recyclability was confirmed by the photocatalyst efficiency for the GG-$CdMgFe_2O_4$ @TiO_2 nanocomposite, which dropped from 94 % to 87 % for ES and 88 % to 80 % for DDE as shown in Fig. 10**a**. Under the same condition, the biogenic Fe-based nanocatalyst was successfully employed nine times in a row without losing any of its photocatalytic effectiveness or ability to generate active species. However, the very little decrease in the pesticide degradation % noted in each subsequent round might be due to washing. In addition, after nine cycles, pesticides can be coated on the surface of conglomerate NPs, blocking the active areas for photon absorption and resulting in less degradation. The PXRD spectra of biogenic GG-$CdMgFe_2O4$ @TiO_2 following rounds three, five, and nine confirmed that the structure of the biogenic nanocomposites remained unchanged as shown in Fig. 10**b**. To confirm the stability of the nanocomposite even further, atomic absorption spectroscopy is used to check for Cd^{2+} ions in the photodegraded pesticide solution following each round. The lack of measurable levels of leached Cd^{2+} in the experimental solution suggests that the Fe-based biogenic NPs exhibited remarkable stability during the photodegradation of pesticides and also indicates that lattice structural deformation was absent for nine cycles, so confirming the catalyst's recyclability potential in a real-world application [182].

Somanathan et al. investigated the degradation efficiency of a *Calotropis gigantean* extract-based $Ce_{0.2}Ni_{0.8}Fe_2O_4$ NPs. It was revealed that the degradation efficiency reduced significantly after the fifth successful cycle. This was attributed to the blocking of the catalyst's active sites by the reaction by-products[201]. Similarly, Rani and coworkers design Fe_2O_3 NPs from a biochar (BC) synthesized from Citrus limetta peel to fabricate BC@Fe_2O_3 as photocatalyst for degradation of Endosulfan (ES) and Ethion (ET) from the wastewater in acidic medium under natural sunlight. The degradation efficiency of ES and ET are 94 % and 91 % respectively. BC@Fe_2O_3 was reused for seven

Table 3
Overview of recyclability study.

Biosynthesized iron-based NPs	Biogenic source	OC and OP	Eluent	DE @ n = 1	Cycle no	DE @ nth cycle	References
Fe	*Nephelium lappaceum* fruit peel	Endosulfan	Distilled H_2O and n-hexane	94	5	> 85	[172]
$CdMgFe_2O_4$ @TiO_2	Guar gum	Endosulfan	Distilled water and acetone	94	8	87	[182]
BC@ β-FeOOH	*Citrus limetta* waste peels	Endosulfan	Distilled water and acetone	80	8	78	[187]
Fe	*Nephelium lappaceum* fruit peel	Hexachlorobenzene	Distilled H_2O and n-hexane	95	5	> 85	[172]
Citrus limetta BC@ Fe_2O_3	green tea extract	Ethion	Centrifugation, water and acetone	91	7	86	[183]
$CuFe_2O_4$	Arabic Gum-grafted-polyamidoxime	Chlorpyrifos	Ethanol	89.7	3	85.01	[181]
Fe	*Nephelium lappaceum* fruit peel	Heptachlor	Distilled H_2O and n-hexane	97	5	> 90	[172]
BC@ β-FeOOH	*Citrus limetta* waste peels	DDD	Distilled water and acetone	76	8	72	[187]
Citrus limetta BC@ Fe_2O_3	Green tea extract	Endosulfan	Centrifugation, water and acetone	94	7	87	[183]
Fe	*Nephelium lappaceum* fruit peel	Aldrin	Distilled H_2O and n-hexane	97	5	> 90	[172]
$CdMgFe_2O_4$ @TiO_2	Guar gum	DDE	Distilled water and acetone	88	8	80	[182]
Fe	*Nephelium lappaceum* fruit peel	o,p′-DDT	Distilled H_2O and n-hexane	98	5	> 90	[172]
BC@ α-FeOOH	*Citrus limetta* waste peels	DDD	Distilled water and acetone	92	8	90	[187]
Fe	*Nephelium lappaceum* fruit peel	p,p′-DDT	Distilled H_2O and n-hexane	98	5	> 90	[172]
BC@ α-FeOOH	*Citrus limetta* waste peels	Endosulfan	Distilled water and acetone	98	8	95	[187]

consecutive reaction cycles without loss of photocatalytic properties. Notably, up to the seventh round, the PXRD study supported the usage of biosynthesized Fe-base NP in succession and indicated that despite multiple recyclability, there was no discernible structural or lattice deformation in the biogenic NP [183]. Biogenic-based heterogeneous photocatalyst regeneration usually involves washing, centrifugation, and subsequent drying of the catalyst. The magnetic property of biogenic FeNP photocatalysts simplifies their reusability using external magnets to remove the catalysts from the reaction mixture, wash, and reuse [201].

In another study[186], for the photocatalytic degradation of Endosulfan and Atrazine using biosynthesized BC@$NiFe_2O_4$ the stability and recyclability potential of the biogenic NP was evaluated. This was done by using centrifugation to separate and recover the spent biogenic catalyst. The spent biogenic nanocatalyst was then repeatedly washed with acetone and deionized H_2O to get rid of any contaminants that could have adhered to its surface. Before being employed in the following recyclability experiment, the catalyst was dried at 60 °C in a hot air oven. The nanocatalyst was then reused under the same optimal conditions. As shown in Fig. 11**b,** it was discovered that the photocatalytic degradation percentage had altered a little for AT and ES, going from 98 % to 88 % and 92 % to 86 %, respectively. The author opined that the Aggregation of AT and ES onto the nanocatalyst surface may be the cause of a minor drop in the reported % degradation. Additionally, it was observed that the biogenic nanocatalyst structure had not changed significantly as shown in Fig. 11**a**. PXRD analysis was performed to confirm the photocatalyst stability, and small variations in angle or intensity confirmed the catalyst's capacity to be recycled. After the eighth cycle, there was a little drop in BC@$NiFe_2O4$'s efficiency. Because the active areas that initiated the degradation event were occluded after the eighth cycle, photodegradation effectiveness decreased. The regenerated nanocatalyst's reduced performance is probably due to the un-desorbed ES and AT' blocking of the nanocatalyst's active sites and the passivation of the nanocatalyst during the regeneration process. These results offer compelling proof of the biogenic Fe-based nanocatalyst's stability[186]. A comparable recyclability performance and explanation were also accentuated for the photocatalytic degradation of Endosulfan and DDD using biosynthesized BC@ α and β-FeOOH[187]. As shown in the PXRD analysis displayed in Fig. 12**,** the authors established that there was no lattice structural distortion following the recyclability test and this confirms the stability of the biogenic Fe-based NP [187].

Generally, biogenic-based photocatalysts can be reused for up to five or six consecutive reaction cycles without any significant loss in photocatalytic properties[202]. The summary of previously reported photocatalytic degradation of organochlorine and organophosphate using biogenic-based FeNPs photocatalysts is presented in Table 3 below.

12. Key challenges and future perspectives

To be perfectly frank, this study has revealed that biosynthesized Fe-based NPs are an excellent eco-benign photocatalyst for the degradation of OP and OC. However, a few challenges and promising research gaps that can serve as areas for future exploration by researchers were discovered and highlighted below:

One of the first crucial areas for future investigation is an industrial scale and real-life scenario photocatalytic degradation most of the present studies were carried out on a laboratory scale, and this is important for the long-term viability and general adoption of biogenic Fe-based nanoparticles. Additionally, there is a dearth of studies on the regeneration and recyclability of biogenic Fe-based NPs as only a very few works are available in this very important operation. Thus, it is advised that future researchers concentrate their attention and energies on the recovery, regeneration, and recycling of spent degraders as this will confer more eco-economical honor on the use of biogenic Fe-based NPs for the degradation

of many organic pollutants beyond OP and OC. Because the cost of fabricating new NPs often will be reduced or eliminated and this will motivate industries that are interested in wastewater treatment. Additionally, after being recycled several times, it is not recommended to release wasted biogenic Fe-based NPs back into the environment as this will defeat the original purpose of win-win environmental pollution mitigation. Therefore, in our opinion, future studies can examine the circular economy element of discarded biogenic Fe-based NPs and possibly even reuse them to create materials like super-capacitors even after they have been recycled several times in the process of pollutant degradation. Moreover, as there hasn't been a thorough investigation into the ecological impact and long-term stability of biogenic Fe-based nanoparticle applications, researchers ought to take this very seriously. Moreover, scant research has been conducted on the fate, leaching capacity, and secondary impact(s) of biogenic Fe-based NPs following their application for degradation. This is important because if their usage is expanded industrially, things might soon get out of hand. New research on genetically altered organisms is needed to enhance the production of certain reducing molecules and reductants, which control the size and architecture of the biogenic Fe-based NPs[203] for better photocatalytic activities. A critical area for future research would be the creation of a set of guidelines to aid in the programming of the bio-fabrication of biogenic Fe-based NPs and the systematic investigation of the roles played by each component of biological synthesis (DNA sequence, cloning, protein molecule expression, etc.) in the biosynthesis process[203]. We also believe that integrating AI-assisted theoretical methods to support the evaluation of experimental properties of Iron nanoparticles will significantly enhance the robustness of synthetic pathways in the bottom-up approach, enabling the production of large quantities of the nanoparticles. The incorporation of artificial intelligence can provide predictive models and simulations that guide experimental design, optimize reaction conditions, and improve the efficiency and scalability of nanoparticle synthesis. By leveraging AI, researchers can achieve more precise control over the size, shape, and composition of Iron nanoparticles, leading to more consistent and high-quality outcomes. This approach not only accelerates the development process but also reduces the reliance on trial-and-error methods, making the production of Iron nanoparticles more cost-effective and sustainable on an industrial scale. In addition, ultra-structural experimental methods like atom probe tomography and combined spectroscopic techniques with electron tomographic technique would enrich single particle analysis with a high degree of precision and might be applied in future studies [204]. From an economic and environmental protection standpoint, it is crucial to develop a multi-functional surface modifier for iron nanoparticles. This modifier should be designed to maintain the nanoparticles' unique physical and chemical properties, ensuring their enhanced effectiveness in various applications. Additionally, the surface modifier must be readily biodegradable in the soil environment to minimize long-term ecological impact. It should also be free of any hazardous substances to ensure safety for both the environment and human health. Such a development would not only enhance the practical utility of iron nanoparticles but also align with sustainable and environmentally friendly practices, promoting broader acceptance and application of nanotechnology [54]. Furthermore, future research endeavours can explore the possibility of hybrid technology for application optimization by combining photocatalytic degradation with other wastewater remediation techniques. We believe this can deliver better degradation performance synergistically. Finally, given that industrial engineers and investors find this to be a significant issue, financial evaluation is suggested for further research on the production of biogenic Fe-based nanoparticles and their use in OP and OC degradation.

13. Conclusion

Details of photocatalytic degradation of OP and OC by biogenic Fe-based NPs are presented in this review including biogenic Fe-based NPs performance, photocatalytic degradation mechanism, effect of experimental variable, water insecurity overview till 2025, sources and deadly health impact of OP and OC pollutant, and regeneration and reusability studies. These contents are critically and pragmatically reviewed according to recently published peer-reviewed works.

Based on this review, some interesting conclusions were derived. Biogenic Fe-based NPs have been shown to achieve > 80 % OP and OC mineralization and this is suspected to be a result of the exclusive novelty of biogenic iron-based NPs such as excellent regenerability, strong redox potential, ability to absorb a wide range of visible light, and the ability to produce highly reactive oxygen species that can enhance degradation efficiency and low aggregation which are beneficial for the remediation of water contaminants. Moreover, the ability of biogenic iron nanoparticles to maintain stability and reactivity under various environmental conditions makes them a promising solution for environmental cleanup efforts. Findings also show that biogenic iron NPs compete head-to-head and shoulder-to-shoulder as per photocatalytic degradation efficiency. Mechanistically speaking, it was shown that the formation of the oxidizing capability of biogenic Fe-based NPs for the photocatalytic breakdown of OP and OC was significantly influenced by $^{\bullet}OH$ and $O_2^{\bullet}$. It was also revealed that the most prevalent end mineralization products are CO_2 and H_2O, and the least degradation time required is 5 min under 80 W Hg-lamp irradiations for 0.5 μg/L chlorpyrifos-methyl at pH 7. Plant extract is the most often applied reductant for the bio-fabrication of iron and iron oxide NPs. Factors such as temperature, pH, initial concentration of OP and OC, contact/exposure time, and degrader dose have been shown to affect the photocatalytic degradation performance of biogenic Fe-based NPs. The results further showed that the regenerated biogenic Fe-based NPs could be reused for up to seven cycles with over 85 % recovery of pollutants and over 75 % degrading efficiency, provided that the nth regeneration cycle was documented in most degradation tests. Their exceptional reusability marks a significant advancement resulting from ongoing research and development efforts. This progress is largely due to their outstanding magnetic properties, among other unique characteristics mentioned earlier, which enhance their effectiveness and practicality in photocatalysis. In the end, we recommend areas for future work such as circular economy, financial analysis, artificial intelligence integration, and hybrid technology implementation. In conclusion, this study suggests that biogenic Fe-based NPs can be used as a recyclable, environmentally friendly green photocatalyst in real-world scenarios to mineralize and decontaminate various OP and OC contaminants from aquatic ecosystems. This will enable the implementation of robust and viable water security and runoff treatment plans.

CRediT authorship contribution statement

Ademidun Adeola Adesibikan: Writing – review & editing, Writing – original draft, Validation. **Mfeuter Joseph Tachia:** Writing – original draft, Validation. **Kingsley O. Iwuozor:** Writing – review & editing, Writing – original draft, Validation. **Stephen Sunday EMMANUEL:** Writing – review & editing, Writing – original draft, Validation, Methodology, Conceptualization. **Sodiq Adeyeye Nafiu:** Writing – review & editing, Writing – original draft, Validation. **Ebuka Chizitere Emenike:** Writing – review & editing, Writing – original draft, Validation. **Adewale George Adeniyi:** Writing – review & editing, Validation, Supervision, Project administration.

Data Availability

No data was used for the research described in the article.

Declaration of Competing Interest

The authors declare that they have no known competing financial interests or personal relationships that could have appeared to influence the work reported in this paper.

References

[1] du Plessis A, du Plessis A. Global water quality challenges. Freshw Chall South Afr Its Vaal River Curr State Outlook 2017:13–44.

[2] Bănăduc D, Simić V, Cianfaglione K, Barinova S, Afanasyev S, Öktener A, McCall G, Simić S, Curtean-Bănăduc A. Freshwater as a sustainable resource and generator of secondary resources in the 21st century: stressors, threats, risks, management and protection strategies, and conservation approaches. Int J Environ Res Public Health 2022;19:16570.

[3] Jiang Y. China's water security: current status, emerging challenges and future prospects. Environ Sci Policy 2015;54:106–25.

[4] Belhassan K. Water scarcity management. Water Safety, Secur. Sustain. Threat Detect. Mitig. Springer,; 2021. p. 443–62.

[5] Ehtisham M, Badawi AK, Khan AM, Khan RA, Ismail B. Exploring moisture adsorption on cobalt-doped ZnFe 2 O 4 for applications in atmospheric water harvesting. RSC Adv 2024;14:6165–77.

[6] United Nations Development Programme, Water | United Nations Development Programme, (2023). 〈https://www.undp.org/water〉.

[7] Barati AA, Pour MD, Sardooei MA. Water crisis in Iran: A system dynamics approach on water, energy, food, land and climate (WEFLC) nexus. Sci Total Environ 2023;882:163549.

[8] McNally A, Verdin K, Harrison L, Getirana A, Jacob J, Shukla S, Arsenault K, Peters-Lidard C, Verdin JP. Acute water-scarcity monitoring for Africa. Water 2019;11:1968.

[9] Veldkamp TIE, Wada Y, Aerts J, Döll P, Gosling SN, Liu J, Masaki Y, Oki T, Ostberg S, Pokhrel Y. Water scarcity hotspots travel downstream due to human interventions in the 20th and 21st century. Nat Commun 2017;8:1–12.

[10] A. Panhwar, R. Abro, A. Kandhro, A.R. Khaskheli, N. Jalbani, K.A. Gishkori, A.M. Mahar, S. Qaisar, Global Water Mapping, Requirements, and Concerns over Water Quality Shortages, (2022).

[11] Emmanuel SS, Adesibikan AA, Opatola EA, Olawoyin CO. A pragmatic review on photocatalytic degradation of methyl orange dye pollutant using greenly biofunctionalized nanometallic materials: A focus on aquatic body. Appl Organomet Chem 2023;3:e7108. https://doi.org/10.1002/aoc.7108.

[12] Fida M, Li P, Wang Y, Alam SMK, Nsabimana A. Water contamination and human health risks in Pakistan: a review. Expo Heal 2023;15:619–39.

[13] Kannan M, Bojan N, Swaminathan J, Zicarelli G, Hemalatha D, Zhang Y, Ramesh M, Faggio C. Nanopesticides in agricultural pest management and their environmental risks: A review. Int J Environ Sci Technol 2023:1–26.

[14] Zuo W, Lin Q, Liu X, Lv L, Zhang C, Wu S, Cheng X, Yu Y, Tang T. Spatio-temporal distribution of organochlorine pesticides in agricultural soils of southeast China during 2014-2019. Environ Res 2023:116274.

[15] Adeyi AA, Babalola B, Akpotu SO. Occurrence, distribution, and risk of organochlorine pesticides in food and greenness assessment of method. Environ Sci Pollut Res 2021;28:33433–44.

[16] Bhattu M, Kathuria D, Billing BK, Verma M. Chromatographic techniques for the analysis of organophosphate pesticides with their extraction approach: a review (2015–2020). Anal Methods 2022;14:322–58.

[17] Liu X, Wang X, Jiang W, Zhang C-R, Zhang L, Liang R-P, Qiu J-D. Covalent organic framework modified carbon nanotubes for removal of uranium (VI) from mining wastewater. Chem Eng J 2022;450:138062.

[18] Zaghden H, Barhoumi B, Jlaiel L, Guigue C, Chouba L, Touil S, Sayadi S, Tedetti M. Occurrence, origin and potential ecological risk of dissolved polycyclic aromatic hydrocarbons and organochlorines in surface waters of the Gulf of Gabès (Tunisia, Southern Mediterranean Sea). Mar Pollut Bull 2022;180:113737.

[19] Kamalesh T, Kumar PS, Rangasamy G. An insights of organochlorine pesticides categories, properties, eco-toxicity and new developments in bioremediation process. Environ Pollut 2023:122114.

[20] Zhang Y, Zhou B, Chen H, Yuan R. Heterogeneous photocatalytic oxidation for the removal of organophosphorus pollutants from aqueous solutions: A review. Sci Total Environ 2023;856:159048.

[21] Olisah C, Rubidge G, Human LRD, Adams JB. Organophosphate pesticides in South African eutrophic estuaries: Spatial distribution, seasonal variation, and ecological risk assessment. Environ Pollut 2022;306:119446.

[22] Oginawati K, Susetyo SH, Rahmawati SI, Kurniawan SB, Abdullah SRS. Distribution of organochlorine pesticide pollution in water, sediment, mollusk, and fish at Saguling Dam, West Java, Indonesia. Toxicol Res 2021:1–9.

[23] Emmanuel SS, Adesibikan AA, Olawoyin CO, Idris MO. Photocatalytic Degradation of Maxilon Dye Pollutants using Nano-Architecture Functional Materials: A Review. ChemistrySelect 2024;9:e202400316. https://doi.org/10.1002/slct.202400316.

[24] Emmanuel SS, Idris MO, Olawoyin CO, Adesibikan AA, Aliyu AA, Suleiman AI. Biosynthesized Metallic Nanoarchitecture for Photocatalytic Degradation of Emerging Organochlorine and Organophosphate Pollutants: A Review. ChemistrySelect 2024;9:e202304956. https://doi.org/10.1002/slct.202304956.

[25] Emmanuel SS, Adesibikan AA, Bayode AA, Olawoyin CO, Isukuru EJ, Raji OY. A review on covalent organic frameworks with Mult-site functional groups as superior adsorbents for adsorptive sequestration of radio-contaminants. J Organomet Chem 2024;1015:123226. https://doi.org/10.1016/j.jorganchem.2024.123226.

[26] Mali H, Shah C, Raghunandan BH, Prajapati AS, Patel DH, Trivedi U, Subramanian RB. Organophosphate pesticides an emerging environmental contaminant: Pollution, toxicity, bioremediation progress, and remaining challenges. J Environ Sci 2023;127:234–50.

[27] Ugalde-Resano R, Gamboa-Loira B, Mérida-Ortega Á, Rincón-Rubio A, Flores-Collado G, Piña-Pozas M, López-Carrillo L. Exposure to Organochlorine Pesticides and Female Breast Cancer Risk According to Molecular Receptors Expression: a Systematic Review and Meta-analysis of Epidemiological Evidence. Curr Environ Heal Rep 2023:1–17.

[28] Bayode AA, Emmanuel SS, Osti A, Olorunnisola CG, Egbedina AO, Koko DT, Adedipe DT, Helmreich B, Omorogie MO. Applications of perovskite oxides for the cleanup and mechanism of action of emerging contaminants/steroid hormones in water. J Water Process Eng 2024;58:104753. https://doi.org/10.1016/j.jwpe.2023.104753.

[29] Bayode AA, Olisah C, Emmanuel SS, Adesina MO, Koko DT. Sequestration of steroidal estrogen in aqueous samples using an adsorption mechanism: a systemic scientometric review. RSC Adv 2023;13:22675–97.

[30] Badamasi H, Sanni SO, Ore OT, Bayode AA, Koko DT, Akeremale OK, Emmanuel SS. Eggshell waste materials-supported metal oxide nanocomposites for the efficient photocatalytic degradation of organic dyes in water and wastewater: A review. Bioresour Technol Rep 2024;26:101865. https://doi.org/10.1016/j.biteb.2024.101865.

[31] Iwuozor KO, Emenike EC, Gbadamosi FA, Ighalo JO, Umenweke GC, Iwuchukwu FU, Nwakire CO, Igwegbe CA. Adsorption of organophosphate pesticides from aqueous solution: a review of recent advances. Int J Environ Sci Technol 2023;20:5845–94.

[32] Badawi AK, Kriaa K, Osman RM, Hassan R. Modified Rice Husk Waste-Based Filter for Wastewater Treatment: Pilot Study and Reuse Potential. Chem Eng Technol 2024. https://doi.org/10.1002/ceat.202300461.

[33] Jatoi AS, Hashmi Z, Adriyani R, Yuniarto A, Mazari SA, Akhter F, Mubarak NM. Recent trends and future challenges of pesticide removal techniques–a comprehensive review. J Environ Chem Eng 2021;9:105571.

[34] Hassan R, Alluqmani AE, Badawi AK. An Eco-friendly Solution for Greywater Treatment via Date Palm Fiber Filter. Desalin Water Treat 2024:100163.

[35] Matúš P, Littera P, Farkas B, Urík M. Review on Performance of Aspergillus and Penicillium Species in Biodegradation of Organochlorine and Organophosphorus Pesticides. Microorganisms 2023;11:1485.

[36] Badawi AK, Hassan R, Farouk M, Bakhoum ES, Salama RS. Optimizing the coagulation/flocculation process for the treatment of slaughterhouse and meat processing wastewater: experimental studies and pilot-scale proposal. Int J Environ Sci Technol 2024:1–16.

[37] Badawi AK, Salama RS, Mostafa MMM. Natural-based coagulants/flocculants as sustainable market-valued products for industrial wastewater treatment: a review of recent developments. RSC Adv 2023;13:19335–55.

[38] Brovini EM, Moreira FD, Martucci MEP, de Aquino SF. Water treatment technologies for removing priority pesticides. J Water Process Eng 2023;53:103730.

[39] An X, Chen Y, Ao M, Jin Y, Zhan L, Yu B, Wu Z, Jiang P. Sequential photocatalytic degradation of organophosphorus pesticides and recovery of orthophosphate by biochar/α-Fe2O3/MgO composite: A new enhanced strategy for reducing the impacts of organophosphorus from wastewater. Chem Eng J 2022;435:135087.

[40] Ahmad F, Nisar S, Mehmood M. A Critical Review on the Photo Degradation of Diazinon, A Persistent Organic Pesticides. J Chem Soc Pak 2022;44.

[41] Al Alwan B, Ismail B, El Jery A, Badawi AK. State-of-the-art strategies for microplastics mitigation in aquatic environments: Identification, technological innovations, and prospects for advancement. J Water Process Eng 2024;61:105336.

[42] Vaya D, Surolia PK. Semiconductor based photocatalytic degradation of pesticides: An overview. Environ Technol Innov 2020;20:101128.

[43] Bano K, Kaushal S, Singh PP. A review on photocatalytic degradation of hazardous pesticides using heterojunctions. Polyhedron 2021;209:115465.

[44] Meng K, Zhou K, Chang C-T. Ultrasonic Preparation of PN for the Photodegradation of 17β-Estradiol in Water and Biotoxicity Assessment of 17β-Estradiol after Degradation. Catalysts 2023;13:332.

[45] Huang L, Huang X, Yan J, Liu Y, Jiang H, Zhang H, Tang J, Liu Q. Research progresses on the application of perovskite in adsorption and photocatalytic removal of water pollutants. J Hazard Mater 2023;442:130024.

[46] Ye J, Liu J, Li C, Zhou P, Wu S, Ou H. Heterogeneous photocatalysis of tris (2-chloroethyl) phosphate by UV/TiO2: degradation products and impacts on bacterial proteome. Water Res 2017;124:29–38.

[47] Gholami D, Shahbazi S, Mosleh S, Ghoorchian A, Hajati S, Dashtian K, Yasin G. In situ growth of CuFeS2/CuS bridged heterojunction catalyst with mixed redox-couple cations for excellent photocatalytic degradation of organophosphate insecticide: CFD and DFT modeling. Chem Eng J 2023;461:141950.

[48] Rani S, Sharma A, Tabasum S, Malik AQ, Chaudhary S, Kumar D, Singh H, Singh PP. Highly Efficient Photocatalytic Properties of La-Doped ZnO over Pristine ZnO for Degradation of 2-Chlorophenol from Aquatic Agriculture Waste. Chem Afr 2023:1–10.

[49] Fazal T, Jazaa Y, Bahadur A, Iqbal S, Shah M, Mahmood S, Badawi AK, Khan AM, Shahzad W, Ismail B. Transformation of refractory ceramic MgAl2O4 into blue light emitting nanomaterials by Sr2+/Cr3+ activation. Mater Sci Eng B 2024;303:117273.

[50] Vasantharaj S, Sathiyavimal S, Senthilkumar P, LewisOscar F, Pugazhendhi A. Biosynthesis of iron oxide nanoparticles using leaf extract of Ruellia tuberosa: antimicrobial properties and their applications in photocatalytic degradation. J Photochem Photobiol B Biol 2019;192:74–82.

[51] Fadillah G, Yudha SP, Sagadevan S, Fatimah I, Muraza O. Magnetic iron oxide/clay nanocomposites for adsorption and catalytic oxidation in water treatment applications. Open Chem 2020;18:1148–66.

[52] Olusegun SJ, Souza TGF, Souza G de O, Osial M, Mohallem NDS, Ciminelli VST, Krysinski P. Iron-based materials for the adsorption and photocatalytic degradation of pharmaceutical drugs: a comprehensive review of the mechanism pathway. J Water Process Eng 2023;51:103457.

[53] Emmanuel SS, Adesibikan AA, Saliu OD, Opatola EA. Greenly biosynthesized bimetallic nanoparticles for ecofriendly degradation of notorious dye pollutants: A review. Plant Nano Biol 2023;3:100024.

[54] Xu W, Yang T, Liu S, Du L, Chen Q, Li X, Dong J, Zhang Z, Lu S, Gong Y. Insights into the Synthesis, types and application of iron Nanoparticles: The overlooked significance of environmental effects. Environ Int 2022;158:106980.

[55] Emmanuel SS, Olawoyin CO, Adesibikan AA, Opatola EA. A Pragmatic Review on Bio-polymerized Metallic Nano-Architecture for Photocatalytic Degradation of Recalcitrant Dye Pollutants. J Polym Environ 2023;32:1–30. https://doi.org/10.1007/s10924-023-02986-9.

[56] Salama RS, Gouda MS, Aboud MFA, Alshorifi FT, El-Hallag AA, Badawi AK. Synthesis and characterization of magnesium ferrite-activated carbon composites derived from orange peels for enhanced supercapacitor performance. Sci Rep 2024;14:8223.

[57] Vargas-Ortiz JR, Gonzalez C, Esquivel K. Magnetic iron nanoparticles: synthesis, surface enhancements, and biological challenges. Processes 2022;10:2282.

[58] Su L, Ma J, Wang J, Jiang W, Zhang W, Yang J. Site-selective exposure of iron nanoparticles to achieve rapid interface enrichment for heavy metals. Chem Commun 2020;56:2795–8.

[59] Mohamed A, Atta RR, Kotp AA, Abo El-Ela FI, Abd El-Raheem H, Farghali A, Alkhalifah DHM, Hozzein WN, Mahmoud R. Green synthesis and characterization of iron oxide nanoparticles for the removal of heavy metals (Cd2+ and Ni2+) from aqueous solutions with Antimicrobial Investigation. Sci Rep 2023;13:7227.

[60] Aragaw TA, Bogale FM, Aragaw BA. Iron-based nanoparticles in wastewater treatment: A review on synthesis methods, applications, and removal mechanisms. J Saudi Chem Soc 2021;25:101280.

[61] Hammad EN, Salem SS, Mohamed AA, El-Dougdoug W. Environmental impacts of ecofriendly iron oxide nanoparticles on dyes removal and antibacterial activity. Appl Biochem Biotechnol 2022;194:6053–67.

[62] Sharma K, Tyagi S, Vikal S, Devi A, Gautam YK, Singh BP. Sustainable nanomaterials for environmental remediation. Handb. Green Sustain. Nanotechnol. Fundam. Dev. Appl. Springer,; 2023. p. 933–71.

[63] Kumar B, Smita K, Cumbal L, Debut A. Biogenic synthesis of iron oxide nanoparticles for 2-arylbenzimidazole fabrication. J Saudi Chem Soc 2014;18:364–9.

[64] Singh SK, Mishra PK, Upadhyay SN. Recent developments in photocatalytic degradation of insecticides and pesticides. Rev Chem Eng 2023;39:225–70.

[65] Daramola IO, Ojemaye MO, Okoh AI, Okoh OO. Occurrence of herbicides in the aquatic environment and their removal using advanced oxidation processes: a critical review. Environ Geochem Health 2023;45:1231–60.

[66] Chaudhari YS, Kumar P, Soni S, Gacem A, Kumar V, Singh S, Yadav VK, Dawane V, Piplode S, Jeon B-H. An inclusive outlook on the fate and persistence of pesticides in the environment and integrated eco-technologies for their degradation. Toxicol Appl Pharmacol 2023:116449.

[67] Bagal MV, Nandgawle BA, Thosar RV, Mohod AV, Gogate PR. Degradation of pesticides using hybrid processes based on cavitation and photocatalysis: A review. Environ Qual Manag 2023.

[68] Shanaah HH, Alzaimoor EFH, Rashdan S, Abdalhafith AA, Kamel AH. Photocatalytic Degradation and Adsorptive Removal of Emerging Organic Pesticides Using Metal Oxide and Their Composites: Recent Trends and Future Perspectives. Sustainability 2023;15:7336.

[69] Alhalili Z. Metal Oxides Nanoparticles: General Structural Description, Chemical, Physical, and Biological Synthesis Methods, Role in Pesticides and Heavy Metal Removal through Wastewater Treatment. Molecules 2023;28:3086.

[70] Dang Y, Tang K, Wang Z, Cui H, Lei J, Wang D, Liu N, Zhang X. Organophosphate Esters (OPEs) Flame Retardants in Water: A Review of Photocatalysis. Adsorpt, Biol Degrad, Mol 2023;28:2983.

[71] Rani M, Shanker U, Jassal V. Recent strategies for removal and degradation of persistent & toxic organochlorine pesticides using nanoparticles: a review. J Environ Manag 2017;190:208–22.

[72] Hadei M, Mesdaghinia A, Nabizadeh R, Mahvi AH, Rabbani S, Naddafi K. A comprehensive systematic review of photocatalytic degradation of pesticides using nano TiO 2. Environ Sci Pollut Res 2021;28:13055–71.

[73] El-Sheikh MA, Hadibarata T, Yuniarto A, Sathishkumar P, Abdel-Salam EM, Alatar AA. Role of nanocatalyst in the treatment of organochlorine compounds-A review. Chemosphere 2021;268:128873.

[74] Khan SH, Pathak B. Zinc oxide based photocatalytic degradation of persistent pesticides: A comprehensive review. Environ Nanotechnol, Monit Manag 2020;13:100290.

[75] de Oliveira R, da Silva Martini W, Sant'Ana AC. Combined effect involving semiconductors and plasmonic nanoparticles in photocatalytic degradation of pesticides, Environ. Nanotechnol, Monit Manag 2022;17:100657.

[76] Kajitvichyanukul P, Nguyen V-H, Boonupara T, Thi L-AP, Watcharenwong A, Sumitsawan S, Udomkun P. Challenges and effectiveness of nanotechnology-based photocatalysis for pesticides-contaminated water: A review. Environ Res 2022;212:113336.

[77] Sud D, Kaur P. Heterogeneous photocatalytic degradation of selected organophosphate pesticides: a review. Crit Rev Environ Sci Technol 2012;42:2365–407.

[78] Tyagi H, Chawla H, Bhandari H, Garg S. Recent-enhancements in visible-light photocatalytic degradation of organochlorines pesticides: A review. Mater Today Proc 2022;49:3289–305.

[79] Patle TK, Kurrey R, Dewangan K, Shrivas K. Degradation, removal, and detection of pesticides using nanocomposites. Multifunct Hybrid Nanomater Sustain Agric-Food Ecosyst 2020:241–54.

[80] Rani M, Shanker U. Degradation of traditional and new emerging pesticides in water by nanomaterials: recent trends and future recommendations. Int J Environ Sci Technol 2018;15:1347–80.

[81] Bruckmann FS, Schnorr C, Oviedo LR, Knani S, Silva LFO, Silva WL, Dotto GL, Bohn Rhoden CR. Adsorption and photocatalytic degradation of pesticides into nanocomposites: a review. Molecules 2022;27:6261.

[82] Emmanuel SS, Adesibikan AA. Bio-fabricated green silver nano-architecture for degradation of methylene blue water contaminant: A mini-review. Water Environ Res 2021;93:2873–82.

[83] Dokhani S, Assadi M, Pollet BG. Techno-economic assessment of hydrogen production from seawater. Int J Hydrog Energy 2023;48:9592–608.

[84] Alawee WH, Hammoodi KA, Dhahad HA, Omara ZM, Essa FA, Abdullah AS, Amro MI. Effects of magnetic field on the performance of solar distillers: a review study. Eng Technol J 2023;41:121–31.

[85] World Economic Forum, World Economic Forum, (2019). 〈https://www.weforum.org/publications/the-global-risks-report-2019〉 (accessed October 25, 2023).

[86] Zhong R, Chen A, Zhao D, Mao G, Zhao X, Huang H, Liu J. Impact of international trade on water scarcity: An assessment by improving the Falkenmark indicator. J Clean Prod 2023;385:135740.

[87] Emmanuel SS, Adesibikan AA, Saliu OD. Phytogenically bioengineered metal nanoarchitecture for degradation of refractory dye water pollutants: A pragmatic minireview. Appl Organomet Chem 2023;37:e6946.

[88] Hong J, Zhang T, Shen X, Zhai Y, Bai Y, Hong J. Water, energy, and carbon integrated footprint analysis from the environmental-economic perspective for apple production in China. J Clean Prod 2022;368:133184.

[89] Dehghani S, Bavani ARM, Roozbahani A, Gohari A, Berndtsson R. Towards an integrated system modeling of water scarcity with projected changes in climate and socioeconomic conditions. Sustain Prod Consum 2022;33:543–56.

[90] Rosinger AY. Water Needs, Water Insecurity, and Human Biology. Annu Rev Anthropol 2023;52.

[91] Young SL, Frongillo EA, Jamaluddine Z, Melgar-Quiñonez H, Pérez-Escamilla R, Ringler C, Rosinger AY. Perspective: the importance of water security for ensuring food security, good nutrition, and well-being. Adv Nutr 2021;12:1058–73.

[92] Jepson WE, Wutich A, Colllins SM, Boateng GO, Young SL. Progress in household water insecurity metrics: a cross-disciplinary approach. Wiley Interdiscip Rev Water 2017;4:e1214.

[93] Wutich A, Budds J, Eichelberger L, Geere J, Harris LM, Horney JA, Jepson W, Norman E, O'Reilly K, Pearson AL. Advancing methods for research on household water insecurity: Studying entitlements and capabilities, socio-cultural dynamics, and political processes, institutions and governance. Water Secur 2017;2:1–10.

[94] Danielaini TT, Maheshwari B, Hagare D. An assessment of household water insecurity in a rapidly developing coastal metropolitan region of Indonesia. Sustain Cities Soc 2019;46:101382.

[95] Workman CL, Ureksoy H. Water insecurity in a syndemic context: Understanding the psycho-emotional stress of water insecurity in Lesotho, Africa. Soc Sci Med 2017;179:52–60.

[96] Wutich A, Ragsdale K. Water insecurity and emotional distress: coping with supply, access, and seasonal variability of water in a Bolivian squatter settlement. Soc Sci Med 2008;67:2116–25.

[97] Eichelberger L. Household water insecurity and its cultural dimensions: preliminary results from Newtok, Alaska. Environ Sci Pollut Res 2018;25:32938–51.

[98] Brewis A, Workman C, Wutich A, Jepson W, Young S, HWISE-RCN HWIECN, Adams E, Ahmed JF, Alexander M, Balogun M. Household water insecurity is strongly associated with food insecurity: evidence from 27 sites in low-and middle-income countries. Am J Hum Biol 2020;32:e23309.

[99] Adams EA, Stoler J, Adams Y. Water insecurity and urban poverty in the Global South: Implications for health and human biology. Am J Hum Biol 2020;32:e23368.

[100] Wutich A, Brewis A, Tsai A. Water and mental health. Wiley Interdiscip Rev Water 2020;7:e1461.

[101] Mehta L. Water and human development. World Dev 2014;59:59–69.

[102] Weststrate J, Dijkstra G, Eshuis J, Gianoli A, Rusca M. The sustainable development goal on water and sanitation: learning from the millennium development goals. Soc Indic Res 2019;143:795–810.

[103] Fleetwood J. Social justice, food loss, and the sustainable development goals in the era of COVID-19. Sustainability 2020;12:5027.

[104] Carrard N, Foster T, Willetts J. Groundwater as a source of drinking water in southeast Asia and the Pacific: a multi-country review of current reliance and resource concerns. Water 2019;11:1605.

[105] Bwire G, Sack DA, Kagirita A, Obala T, Debes AK, Ram M, Komakech H, George CM, Orach CG. The quality of drinking and domestic water from the surface water sources (lakes, rivers, irrigation canals and ponds) and springs in cholera prone communities of Uganda: an analysis of vital physicochemical parameters. BMC Public Health 2020;20:1–18.

[106] UNU-INWEH, Global Water Security 2023 Assessment - World | ReliefWeb, (2023). 〈https://reliefweb.int/report/world/global-water-security-2023-assessment〉.

[107] Khan ST, Malik A. Engineered nanomaterials for water decontamination and purification: From lab to products. J Hazard Mater 2019;363:295–308.

[108] Wen X, Chen F, Lin Y, Zhu H, Yuan F, Kuang D, Jia Z, Yuan Z. Microbial indicators and their use for monitoring drinking water quality—A review. Sustainability 2020;12:2249.

[109] Abedin MA, Collins AE, Habiba U, Shaw R. Climate change, water scarcity, and health adaptation in southwestern coastal Bangladesh. Int J Disaster Risk Sci 2019;10:28–42.

[110] W.H.O., Water | WHO | Regional Office for Africa, (2023). 〈https://www.afro.who.int/health-topics/water〉.

[111] Lubchenco J, Haugan PM. The future of food from the sea. Blue Compend. From Knowl. to Action a Sustain. Ocean Econ. Springer,; 2023. p. 1–13.

[112] Pingali P, Boiteau J, Choudhry A, Hall A. Making meat and milk from plants: A review of plant-based food for human and planetary health. World Dev 2023;170:106316.

[113] Sultan M, Hamid N, Junaid M, Duan J-J, Pei D-S. Organochlorine pesticides (OCPs) in freshwater resources of Pakistan: A review on occurrence, spatial distribution and associated human health and ecological risk assessment. Ecotoxicol Environ Saf 2023;249:114362. https://doi.org/10.1016/j.ecoenv.2022.114362.
[114] Ashesh A, Singh S, Linthoingambi Devi N, Chandra Yadav I. Organochlorine pesticides in multi-environmental matrices of India: A comprehensive review on characteristics, occurrence, and analytical methods. Microchem J 2022;177:107306. https://doi.org/10.1016/j.microc.2022.107306.
[115] Leadprathom N, Parkpian P, Satayavivad J, Delaune RD, Jugsujinda A. Transport and deposition of organochlorine pesticides from farmland to estuary under tropical regime and their potential risk to aquatic biota. J Environ Sci Heal Part B 2009;44:249–61.
[116] Taiwo AM. A review of environmental and health effects of organochlorine pesticide residues in Africa. Chemosphere 2019;220:1126–40. https://doi.org/10.1016/j.chemosphere.2019.01.001.
[117] El Bouraie MM, El Barbary AA, Yehia M. Determination of organochlorine pesticide (OCPs) in shallow observation wells from El-Rahawy contaminated area, Egypt. Environ Res Eng Manag 2011;57:28–38.
[118] Van den Brink PJ. Assessing aquatic population and community-level risks of pesticides. Environ Toxicol Chem 2013;32:972–3.
[119] Kaushal J, Khatri M, Arya SK. A treatise on Organophosphate pesticide pollution: Current strategies and advancements in their environmental degradation and elimination. Ecotoxicol Environ Saf 2021;207:111483.
[120] Ali U, Syed JH, Malik RN, Katsoyiannis A, Li J, Zhang G, Jones KC. Organochlorine pesticides (OCPs) in South Asian region: a review. Sci Total Environ 2014;476:705–17.
[121] Adeyeye SAO, Oyewole OB, Obadina AO, Omemu AM, Adeniran OE, Oyedele HA, Abayomi SO. Quality and safety assessment of traditional smoked fish from Lagos State, Nigeria. Int J Aquac 2015;5.
[122] Shetty SS, Sonkusare S, Naik PB, Madhyastha H. Environmental pollutants and their effects on human health. Heliyon 2023.
[123] Islam MA, Amin SMN, Rahman MA, Juraimi AS, Uddin MK, Brown CL, Arshad A. Chronic effects of organic pesticides on the aquatic environment and human health: A review. Environ Nanotechnol, Monit Manag 2022;18:100740. https://doi.org/10.1016/j.enmm.2022.100740.
[124] Moebus S, Boedeker W. Case Fatality as an Indicator for the Human Toxicity of Pesticides—A Systematic Scoping Review on the Availability and Variability of Severity Indicators of Pesticide Poisoning. Int J Environ Res Public Health 2021;18:8307.
[125] Eddleston M. Poisoning by pesticides. Med (Baltim) 2020;48:214–7.
[126] Boedeker W, Watts M, Clausing P, Marquez E. The global distribution of acute unintentional pesticide poisoning: estimations based on a systematic review. BMC Public Health 2020;20:1–19.
[127] Hassaan MA, El Nemr A. Pesticides pollution: Classifications, human health impact, extraction and treatment techniques. Egypt J Aquat Res 2020;46:207–20. https://doi.org/10.1016/j.ejar.2020.08.007.
[128] Halstead NT, McMahon TA, Johnson SA, Raffel TR, Romansic JM, Crumrine PW, Rohr JR. Community ecology theory predicts the effects of agrochemical mixtures on aquatic biodiversity and ecosystem properties. Ecol Lett 2014;17:932–41.
[129] Cochard R, Maneepitak S, Kumar P. Aquatic faunal abundance and diversity in relation to synthetic and natural pesticide applications in rice fields of Central Thailand. Int J Biodivers Sci Ecosyst Serv Manag 2014;10:157–73.
[130] Ore OT, Adeola AO, Bayode AA, Adedipe DT, Nomngongo PN. Organophosphate pesticide residues in environmental and biological matrices: Occurrence, distribution and potential remedial approaches. Environ Chem Ecotoxicol 2023;5:9–23. https://doi.org/10.1016/j.enceco.2022.10.004.
[131] Wang L, Liu Z, Zhang J, Wu Y, Sun H. Chlorpyrifos exposure in farmers and urban adults: metabolic characteristic, exposure estimation, and potential effect of oxidative damage. Environ Res 2016;149:164–70.
[132] Lin D, Liu Z, Shen R, Chen S, Yang X. Bacterial cellulose in food industry: Current research and future prospects. Int J Biol Macromol 2020;158:1007–19.
[133] Guan K-L, Liu Y, Luo X-J, Zeng Y-H, Mai B-X. Short-and medium-chain chlorinated paraffins in aquatic organisms from an e-waste site: Biomagnification and maternal transfer. Sci Total Environ 2020;708:134840.
[134] Jia Z-Q, Zhang Y-C, Huang Q-T, Jones AK, Han Z-J, Zhao C-Q. Acute toxicity, bioconcentration, elimination, action mode and detoxification metabolism of broflanilide in zebrafish, Danio rerio. J Hazard Mater 2020;394:122521.
[135] Łozowicka B, Kaczyński P, Mojsak P, Rusiłowska J, Beknazarova Z, Ilyasova G, Absatarova D. Systemic and non-systemic pesticides in apples from Kazakhstan and their impact on human health. J Food Compos Anal 2020;90:103494.
[136] Bhandari G, Atreya K, Scheepers PTJ, Geissen V. Concentration and distribution of pesticide residues in soil: Non-dietary human health risk assessment. Chemosphere 2020;253:126594.
[137] Wang X, Zhang Z, Zhang R, Huang W, Dou W, You J, Jiao H, Sun A, Chen J, Shi X. Occurrence, source, and ecological risk assessment of organochlorine pesticides and polychlorinated biphenyls in the water–sediment system of Hangzhou Bay and East China Sea. Mar Pollut Bull 2022;179:113735.
[138] Parween T, Bhandari P, Sharma R, Jan S, Siddiqui ZH, Patanjali PK. Bioremediation: a sustainable tool to prevent pesticide pollution. Mod Age Environ Probl Their Remediat 2018:215–27.
[139] El-Nahhal Y. Pesticide residues in honey and their potential reproductive toxicity. Sci Total Environ 2020;741:139953.
[140] Miranda-Contreras L, Gómez-Pérez R, Rojas G, Cruz I, Berrueta L, Salmen S, Colmenares M, Barreto S, Balza A, Zavala L. Occupational exposure to organophosphate and carbamate pesticides affects sperm chromatin integrity and reproductive hormone levels among Venezuelan farm workers. J Occup Health 2013;55:195–203.
[141] Pardo LA, Beane Freeman LE, Lerro CC, Andreotti G, Hofmann JN, Parks CG, Sandler DP, Lubin JH, Blair A, Koutros S. Pesticide exposure and risk of aggressive prostate cancer among private pesticide applicators. Environ Heal 2020;19:1–12.
[142] Cohn BA, La Merrill M, Krigbaum NY, Yeh G, Park J-S, Zimmermann L, Cirillo PM. DDT exposure in utero and breast cancer. J Clin Endocrinol Metab 2015;100:2865–72.
[143] Ortega Jacome GP, Koifman RJ, Rego Monteiro GT, Koifman S. Environmental exposure and breast cancer among young women in Rio de Janeiro, Brazil. J Toxicol Environ Heal Part A 2010;73:858–65.
[144] Koutros S, Silverman DT, Alavanja MCR, Andreotti G, Lerro CC, Heltshe S, Lynch CF, Sandler DP, Blair A, Beane Freeman LE. Occupational exposure to pesticides and bladder cancer risk. Int J Epidemiol 2016;45:792–805.
[145] Tang M, Chen K, Yang F, Liu W. Exposure to organochlorine pollutants and type 2 diabetes: a systematic review and meta-analysis. PLoS One 2014;9:e85556.
[146] Sylvie Azandjeme C, Bouchard M, Fayomi B, Djrolo F, Houinato D, Delisle H. Growing burden of diabetes in sub-saharan Africa: contribution of pesticides? Curr Diabetes Rev 2013;9:437–49.
[147] El-Nahhal I, El-Nahhal Y. Pesticide residues in drinking water, their potential risk to human health and removal options. J Environ Manag 2021;299:113611.
[148] Di Bella G, Licata P, Bruzzese A, Naccari C, Trombetta D, Lo Turco V, Dugo G, Richetti A, Naccari F. Levels and congener pattern of polychlorinated biphenyl and organochlorine pesticide residues in bluefin tuna (Thunnus thynnus) from the Straits of Messina (Sicily, Italy). Environ Int 2006;32:705–10.
[149] Miodovnik A, Edwards A, Bellinger DC, Hauser R. Developmental neurotoxicity of ortho-phthalate diesters: review of human and experimental evidence. Neurotoxicology 2014;41:112–22.
[150] Qi S-Y, Xu X-L, Ma W-Z, Deng S-L, Lian Z-X, Yu K. Effects of organochlorine pesticide residues in maternal body on infants. Front Endocrinol (Lausanne) 2022;13:890307.
[151] Hood RB, Liang D, Chiu Y-H, Sandoval-Insausti H, Chavarro JE, Jones D, Hauser R, Gaskins AJ. Pesticide residue intake from fruits and vegetables and alterations in the serum metabolome of women undergoing infertility treatment. Environ Int 2022;160:107061.
[152] Olisah C, Okoh OO, Okoh AI. Global evolution of organochlorine pesticides research in biological and environmental matrices from 1992 to 2018: A bibliometric approach. Emerg Contam 2019;5:157–67.
[153] Du H, Wang Q, Chen G. Photo/electro-catalytic degradation of micro-and nanoplastics by nanomaterials and corresponding degradation mechanism. TrAC Trends Anal Chem 2022:116815.
[154] Ramakrishnan B, Venkateswarlu K, Sethunathan N, Megharaj M. Local applications but global implications: Can pesticides drive microorganisms to develop antimicrobial resistance? Sci Total Environ 2019;654:177–89.
[155] Ross GW, Abbott RD, Petrovitch H, Duda JE, Tanner CM, Zarow C, Uyehara-Lock JH, Masaki KH, Launer LJ, Studabaker WB. Association of brain heptachlor epoxide and other organochlorine compounds with lewy pathology. Mov Disord 2019;34:228–35.
[156] Iwuozor KO, Umeh CT, Emmanuel SS, Emenike EC, Egbemhenghe AU, Ore OT, Micheal TT, Omoarukhe FO, Sagboye PA, Ojukwu VE. A comprehensive review on the sequestration of dyes from aqueous media using maize-/corn-based adsorbents. Water Pract Technol 2023;18:3065–108.
[157] Kumar B, Smita K, Galeas S, Sharma V, Guerrero VH, Debut A, Cumbal L. Characterization and application of biosynthesized iron oxide nanoparticles using Citrus paradisi peel: A sustainable approach. Inorg Chem Commun 2020;119:108116.
[158] Begum SJP, Pratibha S, Rawat JM, Venugopal D, Sahu P, Gowda A, Qureshi KA, Jaremko M. Recent advances in green synthesis, characterization, and applications of bioactive metallic nanoparticles. Pharmaceuticals 2022;15:455.
[159] Ansari M, Ahmed S, Abbasi A, Khan MT, Subhan M, Bukhari NA, Hatamleh AA, Abdelsalam NR. Plant mediated fabrication of silver nanoparticles, process optimization, and impact on tomato plant. Sci Rep 2023;13:18048.
[160] Kurhade P, Kodape S, Choudhury R. Overview on green synthesis of metallic nanoparticles. Chem Pap 2021;75:5187–222.
[161] Jadoun S, Chauhan NPS, Zarrintaj P, Barani M, Varma RS, Chinnam S, Rahdar A. Synthesis of nanoparticles using microorganisms and their applications: A review. Environ Chem Lett 2022;20:3153–97.
[162] Ramrakhiani L, Ghosh S. Metallic nanoparticle synthesised by biological route: safer candidate for diverse applications. IET Nanobiotechnology 2018;12:392–404.
[163] R. Álvarez-Chimal, J.Á. Arenas-Alatorre, Green synthesis of nanoparticles. A biological approach, (2023).
[164] Khandel P, Shahi SK. Mycogenic nanoparticles and their bio-prospective applications: current status and future challenges. J Nanostructure Chem 2018;8:369–91.
[165] Kiran GS, Nishanth LA, Priyadharshini S, Anitha K, Selvin J. Effect of Fe nanoparticle on growth and glycolipid biosurfactant production under solid state culture by marine Nocardiopsissp. MSA13A. BMC Biotechnol 2014;14:1–10.
[166] Harshiny M, Iswarya CN, Matheswaran M. Biogenic synthesis of iron nanoparticles using Amaranthus dubius leaf extract as a reducing agent. Powder Technol 2015;286:744–9.
[167] Pattanayak M, Nayak PL. Green synthesis and characterization of zero valent iron nanoparticles from the leaf extract of Azadirachta indica (Neem). World J Nano Sci Technol 2013;2:6–9.
[168] Mehrotra N, Tripathi RM, Zafar F, Singh MP. Catalytic degradation of dichlorvos using biosynthesized zero valent iron nanoparticles. IEEE Trans Nanobioscience 2017;16:280–6.

[169] Ningthoujam R, Sahoo B, Ghosh P, Shivani A, Ganguli P, Chaudhuri S. Green production of zero-valent iron nanoparticles using pomegranate peel extracts and its use in lindane degradation. Nanotechnol Environ Eng 2023:1–9.
[170] Nnaji JC, Amaku JF, Amadi OK, Nwadinobi SI. Evaluation and remediation protocol of selected organochlorine pesticides and heavy metals in industrial wastewater using nanoparticles (NPs) in Nigeria. Sci Rep 2023;13:2170.
[171] Díez AM, Fernandes VC, Moreira MM, Pazos M, Sanromán MA, Albergaria T, Delerue-Matos C. Nano-zero-valent particles synthesized with agroindustry wastes for pesticide degradation under real conditions. Process Saf Environ Prot 2023;176:1089–100. https://doi.org/10.1016/j.psep.2023.06.089.
[172] Batool S, Shah AA, Abu Bakar AF, Maah MJ, Abu Bakar NK. Removal of organochlorine pesticides using zerovalent iron supported on biochar nanocomposite from Nephelium lappaceum (Rambutan) fruit peel waste. Chemosphere 2022;289:133011. https://doi.org/10.1016/j.chemosphere.2021.133011.
[173] Yan J, Hu L, Gao W, Yang L, Qian L, Han L, Chen M. Remediation of 1,2-dichlorobenzene contaminated soil by activated persulfate using green synthesized nanoscale zero valent iron: activation mechanism and degradation pathways. J Soils Sediment 2022;22:1135–44. https://doi.org/10.1007/s11368-021-03116-5.
[174] Weng X, Ma L, Guo M, Su Y, Dharmarajan R, Chen Z. Removal of doxorubicin hydrochloride using Fe3O4 nanoparticles synthesized by euphorbia cochinchinensis extract. Chem Eng J 2018;353:482–9.
[175] Prasad C, Yuvaraja G, Venkateswarlu P. Biogenic synthesis of Fe3O4 magnetic nanoparticles using Pisum sativum peels extract and its effect on magnetic and Methyl orange dye degradation studies. J Magn Magn Mater 2017;424:376–81.
[176] Bagheri AR, Ghaedi M, Asfaram A, Bazrafshan AA, Jannesar R. Comparative study on ultrasonic assisted adsorption of dyes from single system onto Fe3O4 magnetite nanoparticles loaded on activated carbon: Experimental design methodology. Ultrason Sonochem 2017;34:294–304.
[177] Althumayri K, Guesmi A, Abd El-Fattah W, Khezami L, Soltani T, Ben Hamadi N, Shahat A. Effective Adsorption and Removal of Doxorubicin from Aqueous Solutions Using Mesostructured Silica Nanospheres: Box–Behnken Design Optimization and Adsorption Performance Evaluation. ACS Omega 2023;8:14144–59.
[178] Gemeay AH, Keshta BE, El-Sharkawy RG, Zaki AB. Chemical insight into the adsorption of reactive wool dyes onto amine-functionalized magnetite/silica core-shell from industrial wastewaters. Environ Sci Pollut Res 2020;27:32341–58.
[179] El-Said WA, Fouad DM, Ali MH, El-Gahami MA. Green synthesis of magnetic mesoporous silica nanocomposite and its adsorptive performance against organochlorine pesticides. Int J Environ Sci Technol 2018;15:1731–44.
[180] Pushkar B, Sevak P. Adsorption study of green synthesized Fe-oxide nanoparticle for DDT removal. Int J Pharm Sci Rev Res 2019;55:84–90.
[181] Hassanzadeh-Afruzi F, Maleki A, Zare EN. Efficient remediation of chlorpyrifos pesticide from contaminated water by superparamagnetic adsorbent based on Arabic gum-grafted-polyamidoxime. Int J Biol Macromol 2022;203:445–56.
[182] Keshu, Rani M, Shanker U. Highly efficient removal of endocrine disrupting pesticides by metal ferrites loaded Guar gum based green nanomaterials. J Mol Liq 2023;387:122611. https://doi.org/10.1016/j.molliq.2023.122611.
[183] Rani M, Keshu, Ankit, Shanker U. Green Synthesis of a Biochar-Based Iron Oxide Catalyst for Efficient Degradation of Pesticides: Kinetics and Photoactivity. ChemistrySelect 2023;8:e202300270.
[184] Sahoo JK, Aniket K, Juhi R, Tanuja M, Priyabrat D, Harekrushna S. Guar gum-coated iron oxide nanocomposite as an efficient adsorbent for Congo red dye. Desalin Water Treat 2017;95:342–54.
[185] Balachandramohan J, Anandan S, Sivasankar T. A simple approach for the sonochemical synthesis of Fe3O4-guargum nanocomposite and its catalytic reduction of p-nitroaniline. Ultrason Sonochem 2018;40:1–10.
[186] Rani M, Keshu, Shanker U. Green construction of biochar@NiFe2O4 nanocomposite for highly efficient photocatalytic remediation of pesticides from agriculture wastewater. Chemosphere 2024;352:141337. https://doi.org/10.1016/j.chemosphere.2024.141337.
[187] Rani M, Ankit, Keshu, Shanker U. Efficient degradation of endocrine disruptor pesticides by biochar iron oxide-based nanocomposite: green synthesis, kinetics, and photoactivity, Biomass Convers. Biorefinery 2023:1–16.
[188] Khalid NR, Majid A, Tahir MB, Niaz NA, Khalid S. Carbonaceous-TiO2 nanomaterials for photocatalytic degradation of pollutants: A review. Ceram Int 2017;43:14552–71. https://doi.org/10.1016/j.ceramint.2017.08.143.
[189] Choudhary S, Rani M, Keshu, Shanker U. Green biosynthesized N-doped Bi2O3@SnO2 nanocomposite for efficient remediation of endocrine disrupting pesticides. Environ Nanotechnol, Monit Manag 2022;18. https://doi.org/10.1016/j.enmm.2022.100746.
[190] Kumar B. Green synthesis of gold, silver, and iron nanoparticles for the degradation of organic pollutants in wastewater. J Compos Sci 2021;5. https://doi.org/10.3390/jcs5080219.
[191] Huang H, Yu D, Hu F, Huang SC, Song J, Chen HY, Li LL, Peng S. Clusters Induced Electron Redistribution to Tune Oxygen Reduction Activity of Transition Metal Single-Atom for Metal–Air Batteries. Angew Chem - Int Ed 2022;61. https://doi.org/10.1002/anie.202116068.
[192] Han M, Zhu S, Lu S, Song Y, Feng T, Tao S, Liu J, Yang B. Recent progress on the photocatalysis of carbon dots: Classification, mechanism and applications. Nano Today 2018;19:201–18. https://doi.org/10.1016/j.nantod.2018.02.008.
[193] Durodola SS, Akeremale OK, Ore OT, Bayode AA, Badamasi H, Olusola JA. A Review on Nanomaterial as Photocatalysts for Degradation of Organic Pollutants. J Fluoresc 2023. https://doi.org/10.1007/s10895-023-03332-x.
[194] Gaur A, Porwal C, Chauhan VS, Vaish R. Synergic effect of photocatalysis and tribocatalysis for dye degradation by BaTiO3 ceramics. J Am Ceram Soc 2024;107:2393–406.
[195] Oluwaniyi OO, Adesibikan AA, Emmanuel SS. Evaluation of Wound-Healing Activity of Securidaca longepedunculata Root Extract in Male Wistar Rats. ChemistrySelect 2022;7:e202200711.
[196] Xu Y, Yin R, Zhang Y, Zhou B, Sun P, Dong X. Unveiling the mechanism of frictional catalysis in water by Bi12TiO20: a charge transfer and contaminant decomposition path study. Langmuir 2022;38:14153–61.
[197] Ruan L, Jia Y, Guan J, Xue B, Huang S, Wang Z, Fu Y, Wu Z. Tribo-electro-catalytic dye degradation driven by mechanical friction using MOF-derived NiCo2O4 double-shelled nanocages. J Clean Prod 2022;345:131060. https://doi.org/10.1016/j.jclepro.2022.131060.
[198] Paknikar KM, Nagpal V, Pethkar AV, Rajwade JM. Degradation of lindane from aqueous solutions using iron sulfide nanoparticles stabilized by biopolymers. Sci Technol Adv Mater 2005;6:370–4.
[199] Aniagor CO, Igwegbe CA, Ighalo JO, Oba SN. Adsorption of doxycycline from aqueous media: A review. J Mol Liq 2021;334:116124. https://doi.org/10.1016/j.molliq.2021.116124.
[200] Joseph A, Vijayanandan A. Photocatalysts synthesized via plant mediated extracts for degradation of organic compounds: A review of formation mechanisms and application in wastewater treatment. Sustain Chem Pharm 2021;22:100453. https://doi.org/10.1016/j.scp.2021.100453.
[201] Somanathan T, Abilarasu A, Jermy BR, Ravinayagam V, Suresh D. Microwave assisted green synthesis Ce0.2Ni0.8Fe2O4 nanoflakes using Calotropis gigantean plant extract and its photocatalytic activity. Ceram Int 2019;45:18091–8. https://doi.org/10.1016/j.ceramint.2019.06.031.
[202] Lu J, Ali H, Hurh J, Han Y, Batjikh I, Rupa EJ, Anandapadmanaban G, Park JK, Yang DC. The assessment of photocatalytic activity of zinc oxide nanoparticles from the roots of Codonopsis lanceolata synthesized by one-pot green synthesis method. Opt (Stuttg) 2019;184:82–9. https://doi.org/10.1016/j.ijleo.2019.03.050.
[203] Emmanuel SS, Adesibikan AA, Olusola Olawoyin C, Bayode AA. A Review of Antithrombolytic, Anticoagulant, and Antiplatelet Activities of Biosynthesized Metallic Nanostructured Multifunctional Materials. ChemistrySelect 2023;8:e202302712. https://doi.org/10.1002/slct.202302712.
[204] Adesibikan AA, Emmanuel SS, Olawoyin CO, Ndungu P. Cellulosic Metallic Nanocomposites for Photocatalytic Degradation of Persistent Dye Pollutants in Aquatic Bodies: A Pragmatic Review. J Organomet Chem 2024:123087. https://doi.org/10.1016/j.jorganchem.2024.123087.